Transcriptomic Profiling Reveals Novel Shear Stress-Sensitive Genes in Human Endothelial Cells

by

Congzhen Qiao

A dissertation submitted in partial fulfillment
of the requirements for the degree of
Doctor of Philosophy
(Pharmacology)
in the University of Michigan
2016

Doctoral Committee:

Professor Y. Eugene Chen, Chair
Professor Daniel T. Eitzman
Professor Lori L. Isom
Professor Richard M. Mortensen

To my extraordinary wife, Xueqing,

my beloved daughter, Amber,

my parents, Haichu and Ying,

and, humbly, to my former mentor, Dr. Benedict R. Lucchesi

ACKNOWLEDGMENTS

I came to Ann Arbor for my Ph.D. training in 2010 as a member of the joint M.D./Ph.D. program between Shanghai Jiao Tong University School of Medicine and the University of Michigan Medical School. I would like to thank Dean Guoqiang Chen, Dr. Gang Huang, Hong Gao, Dean James Woolliscroft, Dr. Joseph Kolars, Dr. Lori Isom, Dr. Victor DiRita, Dr. Ronald Koenig and Dr. Amy Huang for their huge efforts to make this program happen. I would like to thank the Department of Pharmacology, in particular the Chair Dr. Lori Isom and the former Chair Dr. Paul Hollenberg for their unwavering support of students. I thank Dr. William Bill Pratt for his strong faith in me, which motivated me to continue Ph.D. training.

This work would not have been achievable without the support of many individuals, centers and scholarships. I greatly thank Dr. Jifeng Zhang for being a great mentor in experimental design, data analysis and result interpretation; Dr. Meng Fan for his tremendous help in bioinformatic analysis; Dr. Yanbo Fan for his generous sharing of cDNA, plasmids, viruses and guidance of endothelial cell experiments; Dr. Yanhong Guo for her kind advice and support; Dr. Jun Song for his expertise in isolating aorta from rabbit; Haocheng Lu for his generous sharing of plasmids and helping me with mutagenesis experiment.

I must thank my scholarships from Shanghai Jiao Tong University School of Medicine, the Program in Biomedical Science and the Department of Pharmacology at the University of Michigan Medical School, which covered my tuition and stipend for many years.

I am very grateful to my friends and loved ones who have always been supportive throughout the whole time in graduate school. In particular, Yangyang Bao, Bo Wang and Kart Tomberg are the kind of best friends everyone should be lucky enough to have. I cannot be more appreciative to my beloved family, who has always had faith in me and supported me in every way they can to help me with my career, often through their own-sacrifice.

I sincerely appreciate all the support, advice and guidance from my dissertation committee members, Drs. Eugene Chen, Lori Isom, Richard Mortensen and Daniel Eitzman. They have helped me to grow and mature as a scientist. I also would like to thank former committee members, Drs. Benedict Lucchesi and Lou D'Alecy, thank them for nurturing my love of cardiovascular medicine.

Finally, I cannot thank my thesis advisor, Dr. Eugene Chen, enough. Eugene took a chance on a transfer student and gave me full liberty to develop my own projects. He pushed me to work hard since the very first day I joined the lab, encouraged me to discuss experimental designs with experienced assistant professors and post-docs, helped me to reach out to every expertise I might need. His door has always been open to me. I am sincerely grateful for his years of support and insightful advice.

TABLE OF CONTENTS

Page

LIST OF TABLES

LIST OF FIGURES

LIST OF ABBREVIATIONS

EC	Endothelial cell
LS	Laminar shear stress
OS	Oscillatory shear stress
ST	Static culture condition
eNOS	Endothelial NO synthase
PECAM-1	Platelet endothelial cell adhesion molecule-1
VEGFR	Vascular endothelial growth factor receptor
RTK	Receptor-tyrosine kinases
ECM	Extracellular matrix
FAK	Focal adhesion kinases
GPCR	G-protein coupled receptor
MAPK	Mitogen-activated protein kinases
NO	Nitric oxide
ERK	Extracellular signal-regulated kinases
JNK	c-Jun N-terminal kinases
PI3K	Phosphoinositide 3-kinases

PKA	Protein kinase A
MIF	Macrophage migration inhibitory factor
PKC	Protein kinase C
CaMK II	Calcium/calmodulin-dependent protein kinase II
MAPKKK	MAPK kinase kinase
AMP	Adenosine monophosphate
ATP	Adenosine triphosphate
CDK	Cyclin-dependent kinase
MLCK	myosin light chain kinase
ET-1	endothelin-1
PGI_2	Prostaglandin I_2
cGMP	Cyclic guanosine monophosphate
VSMC	Vascular smooth muscle cell
TNF-α	Tissue necrosis factor-α
SREBP	Sterol regulatory element binding proteins
VCAM-1	Vascular cell adhesion molecule 1
VE-cadherin	Vascular endothelial cadherin
mRNA	Messenger RNA
ncRNA	Non-coding RNA
qPCR	Quantitative real-time polymerase chain reaction

HYAL2	Hyaluronoglucosaminidase 2
CXCR4	C-X-C chemokine receptor type 4
ANGPT2	Angiopoietin-2
FABP4	Fatty acid binding protein 4
VCAM1	Vascular cell adhesion molecule 1
ID1	Inhibitor of DNA binding 1
KLF2	Krüppel-like factor 2
KLF11	Krüppel-like factor 11
LMO7	LIM domain 7
TEK	TEK receptor tyrosine kinase, endothelial
SERPINE2	Serpin peptidase inhibitor member 2
C10orf10	Chromosome 10 open reading frame 10
LXN	Latexin
EFNA1	Ephrin-A1
CCL14	Chemokine (C-C motif) ligand 14
NOS3	Nitric oxide synthase 3
IL-1β	Interleukin-1β

CHAPTER I

Introduction: Shear stress and its role in endothelial biology

Overview

The cardiovascular system is persistently exposed to blood flow-generated hemodynamic forces. Hemodynamic forces have been implicated as key factors modeling blood vessel structure, impacting development of cardiovascular diseases such as atherosclerosis, aneurysms and valvular calcification. Shear stress is the frictional force that mainly acts upon the endothelial cell (EC) monolayer within blood vessels. In addition to circulating hormones and key factors, shear stress is critical to endothelial function, maintaining the homeostasis of vasculature. Alterations in the magnitude and direction of shear stress have been evidenced in the pathogenesis of atherosclerosis, which is the major pathological basis of ischemic heart diseases and stroke, the top two causes of death worldwide. In this chapter, I will begin with an introduction of shear stress patterns and location *in vivo*, laying the groundwork for a discussion of the geometrical

distribution of atherosclerosis. I will provide an overview of the effect of biomechanical stimulation on endothelial function/dysfunction and discuss the mechanosensors, signaling pathways, and phenotypical changes both physiologically and pathophysiologically. Possible mechanisms of shear stress-induced atherogenesis will be presented.

Blood flow pattern *in vivo*

Blood flow is an important component of the cardiovascular system. It delivers nutrients and oxygen to every organ for exchange of metabolic wastes and carbon dioxide. It also functions to maintain the pH level, osmotic pressure and body temperature[1]. In addition, the biomechanical characteristics of blood flow heavily participates in vascular physiology. Blood is ejected from a beating heart during systole, while there is no output during diastole under physiological conditions. This cardiac cycle gives rise to the pulsatile shapes of blood flow[1]. The velocity of blood flow and the geometry of blood vessels are the two major components contributing to the blood flow pattern. Multiple blood flow patterns have been observed in the arterial tree (Table 1). Blood flow *in vivo* might be either laminar or turbulent. Laminar blood flow can be further categorized into undisturbed and disturbed laminar flow. The undisturbed laminar blood flow is steady and streamline,

often observed in straight arterial segments with no natural branches or curvatures. Disturbed blood flow, however, is characterized as a reversed or swirling flow, found in areas of curvatures, arterial bifurcations, as well as arterial branches[2]. In contrast to laminar blood flow, turbulent blood flow is rarely present in the arterial tree unless in conditions like aerobic exercise, whereby the velocity of blood flow is increased dramatically or in diseased conditions, such as stenosis[3] and aneurysm[4]. Turbulent blood flow features a continuously changing velocity over time and is distinguished from laminar flow by a high Reynolds (Re) number (>2000), which is defined as the ratio of inertial forces to viscous forces.

Table 1. Blood flow patterns in the arterial tree

Term	Definition	Location
Laminar blood flow	Smooth, steady blood flow	Straight arterial segments with no branching points
Undisturbed laminar blood flow	Smooth, steady blood flow with extremely low Re numbers*	Straight arterial segments with negligible geometric irregularities
Disturbed laminar blood flow	Smooth, reversed blood flow with low Re numbers (<2000)	Arterial segments with curvatures, branches and bifurcations
Turbulent blood flow	Steady blood flow at various flow velocity spatially and temporally with high Re numbers (>2000)	Aortic trunk in conditions like aerobic exercise, segments with severe stenosis and aneurysm
Pulsatile blood flow	Unsteady blood flow in rhythm with the cardiac output	The central arterial tree

*Re numbers = Reynolds numbers, the ratio of inertial forces to viscous forces.

Shear stress types and location

In biomechanics, stress is defined as force intensity per unit area (dyne/cm^2). There are multiple blood flow-related stresses, including cyclic stretch (periodic prolongation of cultured ECs in one or all directions), hydrostatic

pressure (the fluid pressure at equilibrium due to gravity) and fluid shear stress[5].

Fluid shear stress is also known as endothelial shear stress[6] or wall shear stress[7]. It is defined as the frictional force that acts directly upon the luminal surface of the vasculature. Although precise measurement of the magnitude of shear stress *in vivo* is challenging, estimations can be made by Poiseuille's Law, which is used to describe relationships between shear stress and vascular radius, length, blood flow viscosity, and perfusion pressure on the presumption that blood vessels are long and straight as well as that blood flow is steady and laminar conforming to Newtonian fluid mechanics[8]. Shear stress is denoted as τ_s, the magnitude of which can be calculated by equation $\tau_s=4\mu Q/\pi R^3$, where μ is the fluid viscosity, Q is the flow rate and R is the internal radius (Figure 1). Due to the pulsatile nature of blood flow and geometric irregularities of the arterial tree, fluid shear stress *in vivo* is not uniform[7,9].

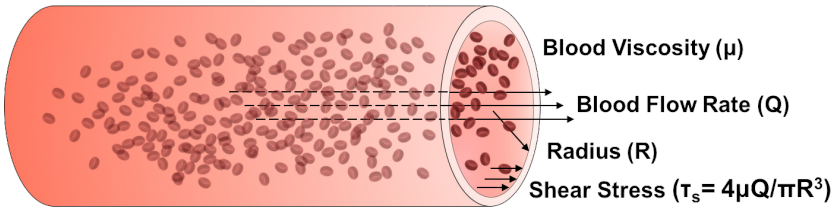

Figure 1. A schematic diagram of a straight artery illustrating elements of fluid shear stress.

In a straight arterial lumen, e.g. in the descending aorta, unidirectional and steady laminar shear stress (LS) is found with a high magnitude ranging from 15-70 dyne/cm^2. In areas of lesser curvatures and arterial bifurcations, low shear stress derived from disturbed blood flow is the predominant one[2]. Given the flow complexity, low shear stress can be further divided into unidirectional low shear stress (<10 dyne/cm^2) and bidirectional oscillatory shear stress (OS) (0~5 dyne/cm^2). Notably, low shear stress occurs more frequently in pathological conditions, such as upstream and downstream of stenoses[1].

Mechanosensors for shear stress

As the only interface between the flowing blood and vascular smooth muscles, the endothelium equipped with numerous mechanosensors acting as the mediator of biomechanical stimulation[10,11]. Various membrane-bound molecules and microdomains have been implicated as potential fluid shear stress detectors and/or transducers, including the membrane phospholipid bilayer, the cytoskeleton, the glycocalyx, primary cilia, adhesion molecules, ion channels, G protein-coupled receptors (GPCR) and receptor-tyrosine kinases[12-16] (Figure 2). The diversity of mechanosensors in the endothelium orchestrates its response to biomechanical stimulation but complicates the

elucidation of underlying mechanisms. Some published studies with insights into molecular mechanisms that regulate the activity and function of mechanosensors are reviewed below.

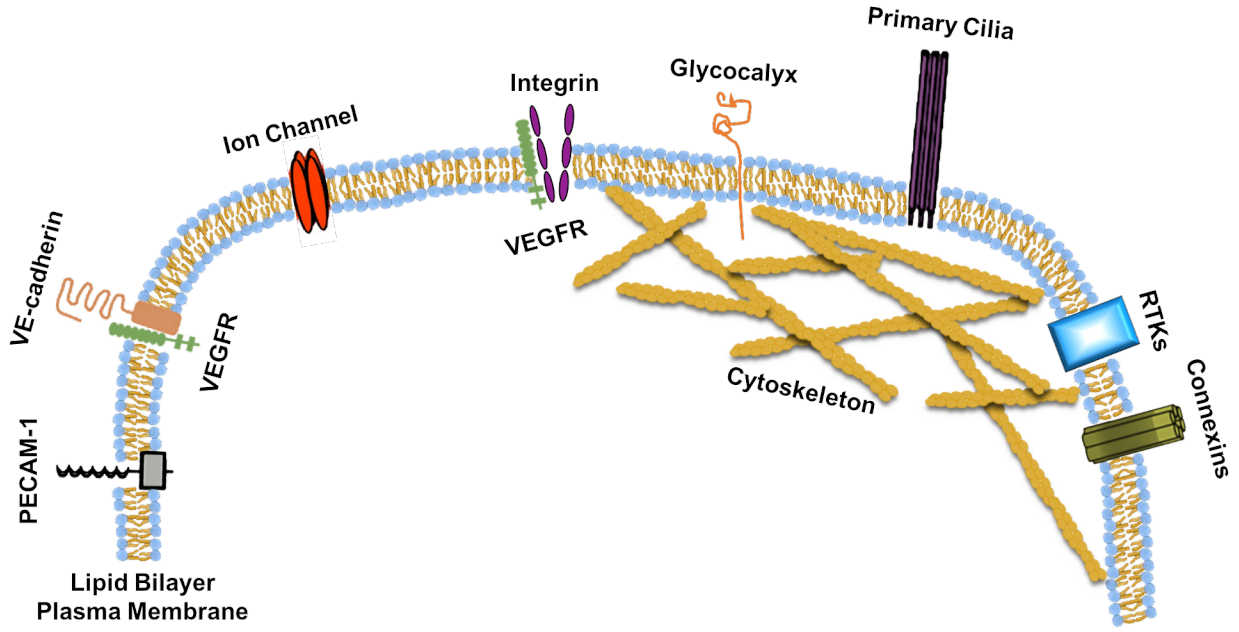

Figure 2. A schematic diagram of mechanosensors for fluid shear stress in endothelium. VE-cadherin, vascular endothelial cadherin; PECAM-1, platelet endothelial cell adhesion molecule-1; VEGFR, vascular endothelial growth factor receptor; RTK, receptor-tyrosine kinase.

Lipid bilayer:

The phospholipid bilayer is the major composition of the plasma membrane. It selectively allows a small variety of ions and molecules in and out of cells to provide protection from extracellular surroundings as well as maintain intracellular homeostasis. Shear stress is believed to increase the permeability of the phospholipid

bilayer[17] and activate the membrane-bound heterotrimeric G proteins in a receptor-independent manner[18]. Butler et al. have demonstrated that shear stress-induced membrane perturbation activates the mitogen-activated protein kinases (MAPKs) signaling pathways[19].

Glycocalyx:

The glycocalyx is a glycoprotein polysaccharide-rich layer that surrounds the cell membrane. The thickness of the layer ranges from 2 μm in small arteries to 4.5 μm in carotid arteries[20,21]. It has been reported to participate in various biological processes including inflammatory response and coagulation[22]. Notably, hyaluronic acid glycosaminoglycan found in the glycocalyx is responsible for LS-induced nitric oxide (NO) production[23].

Primary cilia:

Studies have elucidated that primary cilia play a pivotal role as mechanosensors in the ear, kidney, and developing heart[24]. Interestingly, primary cilia are absent in ECs exposed to LS. Only those located in areas of lesser curvature and arterial bifurcations

are ciliated[25]. Another line of evidence has demonstrated that primary cilia undergo disassembly under LS[26]. Polycystin-1 and polaris, two components of primary cilia, have been implicated as crucial in shear stress-mediated endothelial function[27].

Integrins

Integrins are transmembrane heterodimeric adhesion molecules that belong to a large family of over 20 members. The extracellular domain of integrins binds to the extracellular matrix (ECM) components[28] while the cytoplasmic domain interplays with intracellular molecules to transduce biological signals[14]. Evidence has shown that integrins undergo significant conformational changes in response to shear stress. Binding to ECM ligands is believed to be necessary for this shear stress-induced mechanotransduction of integrins[29], which activates cellular signaling in focal adhesion sites as well as in the cytoskeleton[28,30]. In addition, focal adhesion kinase (FAK) and c-Src, two essential molecules involved in integrin-activated signaling pathways[31,32], are activated by shear stress in ECs[33,34].

Platelet endothelial cell adhesion molecule-1 (PECAM-1)

PECAM-1 is an important adhesion molecule expressed in ECs. It mediates the interaction between ECs and leukocytes and is speculated to function as a mechanosensor in ECs as well. The phosphorylation of PECAM-1 induced by shear stress has been implicated in the activation of Akt and eNOS in ECs[35]. Osawa et al. have shown that once shear force is directly applied to PECAM-1 on the EC surface, PECAM-1 will be rapidly phosphorylated followed by ERK phosphorylation[36].

Ion channels

A large variety of ion channels are expressed in ECs. It is proposed that ion channels are closely involved in shear stress-induced signal transduction[37]. Olesen et al. have identified a non-stretch activated inward-rectifying K^+ current in ECs under fluid shear stress[38]. Hoger et al. have reported that this shear stress-induced K^+ (I_{ks}) current may be activated by endothelial Kir2.1 K^+ channel, which, when expressed in *Xenopus* oocytes or HEK-293 cells, results in an inward rectifying K^+ current similar to the one under fluid shear stress, suggesting its mechanosensing role in ECs. The specific

inactivation of I_{ks} current by genistein suggests that the activation of Kir2.1 channel may be mediated by phosphotyrosine kinase in response to shear stress[39]. In addition to K^+ currents, Ca^{2+} influx increases under LS, suggesting the involvement of calcium channels[37,40].

G-protein coupled receptors (GPCRs)

Mounting evidence indicates that GPCRs are mechanosensors equipped by ECs to detect fluid shear stress. GPCRs are typically activated by ligand binding. Intriguingly, Gudi *et al.* have reported that G proteins can be activated by shear stress via reconstituted lipid bilayer vesicles[18]. In addition, Jo *et al.* have demonstrated that Gi protein inhibitor pertussis toxin blocks shear stress-dependent ERK1/2 activation[41]. Chachisvilis *et al.* have found that fluid shear stress increases the activity of bradykinin B2 GPCR in ECs, which is caused by the conformational changes from inactive form to active form leading to the activation of the receptors[42].

Receptor tyrosine kinases (RTKs)

RTKs are a group of cell surface receptors that transduce signals to maintain normal development and homeostasis[43]. RTKs has been shown to be activated by shear stress[44]. Vascular endothelial growth factor receptor 2(VEGFR2) is a typical RTK on the surface of ECs. It often exists in complexes with other transmembrane proteins, such as VE-cadherin and integrins (Figure 2). Chen *et al.* have demonstrated that VEGFR2 and integrins together can detect and transduce biomechanical stimuli. The transduced signal can be mediated by extracellular signal-regulated kinases (ERK) and c-Jun N-terminal kinases (JNK) pathways[44]. In addition, LS-induced endothelial NO synthase (eNOS) activation has been identified to be mechanotransduced by VEGFR2 in a phosphoinositide 3-kinase (PI3K)/Akt-dependent manner[45].

Shear stress-induced signaling pathways in ECs

ECs are responsible for the maintenance of vascular homeostasis. The complex network of intracellular signaling is important to the involvement of ECs in variety of biological processes, such as inflammation, coagulation, angiogenesis, metabolism, blood pressure maintenance, etc[46]. There is a considerable amount of evidence indicating that shear stress activates a

variety of intracellular signaling pathways in ECs, including MAPKs, PI3K/Akt, FAK, Calcium/calmodulin-dependent protein kinase II (CaMK II), Rho family GTPases, protein kinase A (PKA), protein kinase C-ζ (PKCζ), etc[11,47]. Once activated by fluid shear stress, the mechanosensors transduce biomechanical signals into biochemical activities propagated through the intracellular signaling pathways in ECs[6].

MAPK signaling pathways

MAPKs are heavily involved in cell growth and differentiation as well as extracellular stimuli-induced signal transduction[47]. They serve to phosphorylate downstream kinases and transcription factors at serine/threonine sites. LS has been shown to attenuate MAPK by inhibiting apoptosis signal-regulating kinase 1 (ASK-1), an upstream MAPK kinase kinase (MAPKKK) involved in inflammation signaling[48]. In addition, LS can also activate MAPK phosphatase-1 (MKP-1), which dephosphorylates p38 and JNK to suppress the kinase activities[49]. The transient effect of biomechanical stimulation has also been reported on the intracellular MAPK activation in ECs. Jalali et al. have revealed that LS can activate the p60src-Ras-MAPK signaling pathway to control transcriptional regulation of phorbol ester

TPA-responsive elements and serum-responsive elements through JNK and ERK[34]. Go et al. have published a serious of research findings to demonstrate that shear stress-activated JNK can also be mediated by either PI3K/Akt pathway or its downstream product NO molecule[50-52]. These findings implicate the critical role of MAPK signaling pathways in shear stress-induced mechanotransduction.

PI3K/Akt signaling pathways

PI3K/Akt is an important signaling pathway in modulating various EC functions, including metabolism, cell survival, proliferation and etc[53,54]. PI3Ks receive signals from integrins, RTKs and GPCRs and rapidly produce phosphatidylinositol (3,4,5) trisphosphates (PIP3) to activate downstream Akt cascade. Dimmeler et al. have revealed that LS induces PI3K-mediated Akt phosphorylation in a time-dependent manner, which can be inhibited by PI3K inhibitors wortmannin and Ly294002. This LS-induced Akt phosphorylation potently inhibits ECs apoptosis[55]. In a follow-up study, Go et al. have shown that shear stress activates Ras-JNK pathway via NO, which is produced by PI3K/Akt-phosphorylated endothelial NO synthase (eNOS)[52].

FAK signaling pathways

FAK is a non-receptor tyrosine kinase located in the cytoplasm modulating cell adhesion and motility[56]. At focal adhesion sites, FAK co-localizes with integrins on the intracellular side whereas integrins bind to ECM proteins on the extracellular side. It is well-established that FAK undergoes rapid tyrosine phosphorylation by cell-ECM contact, growth factor-receptor binding and shear stress-triggered cytoskeletal deformation[57]. Studies have shown that FAK is closely involved in integrins-mediated mechanosensing[31]. Li et al have demonstrated that LS increases the FAK phosphorylation and its activity. Furthermore, LS-induced activation of FAK transiently enhances its association with growth factor receptor binding protein 2[33]. FAK of ECs under LS could be rapidly phosphorylated at Tyr925 by Src and activate the downstream MAPKs[58]. In response to LS mechanical force, ECs undergo focal contact remodeling and migrate along the flow direction, where FAK Tyr397 phosphorylation is augmented in migrating cells[59].

CaMK II signaling pathways

CAMK II is universally expressed in various cell types, serves to phosphorylate calcium-dependent proteins in the regulation of cytoskeleton, permeability as well as redox-sensitive regulation in ECs[60]. There are four isoforms of CaMK II, α, β, γ and with δ. High expression of δ and γ are found in ECs[61]. Cai et al. have revealed that CAMK II is the mediator of hydrogen peroxide (H_2O_2)-induced eNOS upregulation[62]. In addition, the same group later has shown that OS may up-regulate intracellular H_2O_2 to activate CAMK II [63] while LS inhibits CAMK II phosphorylation. Thus CAMK II activation may be deleterious regarding endothelial function.

Rho family GTPases signaling pathways

Rho family of GTPases is a subfamily of the Ras superfamily. It consists of 3 subgroups of small GTP-binding proteins, Cdc42, Rac1 and RhoA. Rho family has been well-evidenced in the regulation of cytoskeleton. Furthermore, Rho, Rac and Cdc42 have been reported to regulate separate signal transduction pathways via distinct membrane-bound receptors to regulate the different components of actin cytoskeleton[64,65]. Lin et al. have suggested that LS-induced modulation of sterol regulatory element binding proteins (SREBPs)

activity in ECs depends on the Rho-Rho-associated protein kinase-LIM kinase-cofilin signaling pathways. They've shown that dominant negative mutants of RhoA, ROCK, LIMK, and cofilin can block the LS-induced modulation of SREBPs[66]. Another line of research has reported that LS-activated integrin signaling can induce a transient inhibition of Rho activity, which helps the alignment of ECs with the direction of flow[67]. Mechanistic studies on the specific role of RhoA, Cdc42 and Rac in response to low shear stress has revealed that all three members of Rho family are rapidly activated by low shear stress[68,69]. RhoA can be transiently activated for the first 15 minutes and is responsible for cell rounding whereas Rac1 and Cdc42 activation peaks at 30 minutes and controls the spread and elongation with the direction of flow[69].

PKA signaling pathways

PKA is a cyclic AMP-dependent kinase and is proposed to regulate glycose and lipid metabolism in ECs. The classic pathway of PKA activation involves ligand-GPCR binding, which induces the conformational change of receptor-associated heterotrimeric G protein. The activated Gs alpha subunit binds to adenylyl cyclase to

activate the catalysis of ATP into cyclic AMP, which binds to PKA and exposes its catalytic subunits for protein phosphorylation[70]. PKA has been suggested in biomechanical stimulation-induced EC signaling. Boo et al. have found that LS could induce PKA activation, which phosphorylates eNOS at Ser1179. This process, however, has been shown to be independent of Akt signaling activation[71].

PKC signaling pathways

The PKC isozyme family is a group of multifunctional kinases targeting serine and threonine residues of proteins. PKC can be activated by increased cytosolic diacylglycerol or calcium ion, acting as a critical role in multiple signal transduction pathways[72]. PKC signaling is closely associated with the activation of different receptors including GPCRs, RTKs, etc. to modulate cell proliferation, survival, migration and angiogenesis[73]. PKC has been suggested as a part of the shear stress-induced signaling transduction in ECs. An increase of PKC-β immunostaining has been observed in HUVECs under low shear stress [74]. PKC activity is likely to be induced promptly (<10 min) and declines at 30 min upon exposure to shear stress, but remains higher than the baseline in ECs under static (ST) culture

condition[75]. Another line of evidence has shown that PKC inhibitors, H7 and staurosporine, suppress biomechanical stimulation-induced endothelin-1 expression in ECs[76,77], indicating PKC's essential role in mechanotransduction.

Shear stress-mediated endothelial function and dysfunction

The endothelium is well-recognized as the key to the vascular homeostasis. It interplays with hormones, growth factors and key molecules in the circulating blood to regulate the vascular biology. In addition to the hormonal stimuli, the endothelium is equipped with a large variety of mechanosensors to transduce the hemodynamic forces to downstream effectors for the biomechanical adaptation. Fluid shear stress profoundly changes the morphology as well as the function of ECs. In this part, I will focus on the proliferation, apoptosis, and migration of ECs under different shear stress conditions. A discussion of the potential regulatory mechanisms of EC permeability, alignment and vasoregulation in response to shear stress will be presented as well.

Proliferation

ECs *in vivo* are quiescent in general and the proliferation of ECs is governed by growth factors as well as hemodynamic forces. Ando et al. have observed that low shear stress (0.3-1.7 dyn/cm^2) over 24 hour has significantly increased the proliferation rate of ECs in culture[78]. Levesque et al. have reported that LS inhibits the ECs proliferation in a magnitude-dependent manner[79]. [^{3}H]thymidine incorporation experiment reveals that DNA synthesis of ECs is inhibited by LS. The majority of ECs under LS undergo growth arrest, which is likely due to the p21$^{Sdi1/Cip1/Waf1}$-mediated inhibition of cyclin-dependent kinase 2 and 4. The inactive kinases fail to phosphorylate downstream retinoblastoma protein, which binds to DNA for cell cycle regulation, imprinting LS as anti-proliferative force[80]. Lin et al. have reported that the tumor suppressor p53 is up-regulated by LS in a time and magnitude-dependent manner, which is involved in the LS-induced growth arrest of ECs. LS-triggered mechanotransduction is mediated by JNK phosphorylation of p53[81]. These findings are consistent with in vivo observations that ECs at arterial bifurcations where OS is predominant have a higher turnover rate[82].

Apoptosis

Unlike necrosis, apoptosis of ECs is programmed cell death through defined biochemical interactions. It occurs with caspase cascade activation when the physiological function of ECs is compromised by a wide range of stimuli including hemodynamic forces. It is evidenced that the apoptosis of ECs can be influenced by fluid shear stress[83]. Given the heterogeneity of shear stress distribution *in vivo*, ECs under LS are anti-apoptotic whereas those under OS are pro-apoptotic, predisposing ECs to inflammation. LS has been well-documented to exert vasoprotective effect by increasing the production of NO, which is proposed to protect ECs from apoptosis[84] by nitrosylating caspase-3 at Cys163 to deactivate the caspase cascade[85]. Dimmeler et al. later have revealed that LS activates PI3K/Akt pathway, which is suggested to be involved in the EC apoptosis. By pharmacologically blocking PI3K activity as well as overexpressing dominant negative Akt mutant, they've shown that the LS-suppressed apoptosis is abolished[55]. In contrast, OS generated by disturbed blood flow sensitizes ECs to apoptosis. Heo et al. have provided evidence that peroxynitrite mediated by OS stimulation enhances PKCζ activity in ECs leading to p53 SUMOlation, which, in turn, contributes to EC apoptosis[86]. In vivo

experiments further strengthen the findings that OS contributes to endothelial apoptosis initiation[87].

Migration

Cell migration is a biological process including cell polarization, protrusion formation, adhesion formation and forward movement[88]. It plays a critical role in embryo development, immunoreactivity, wound healing, etc. EC migration is a key step in the process of angiogenesis[89]. A wide range of stimuli has been reported in the regulation of EC migration including fluid shear stress[89]. Albuquerque et al. have performed scratch wound experiments in both HUVECs and HCAECs preconditioned with shear stress and found that LS enhances ECs closure in comparison with those under ST[90].This LS-induced migration is likely to be attributed to the lamellipodia protrusion and focal adhesions remodeling[91]. Multiple lines of evidence have indicated that the small GTPase Rac are essential for the EC migration under LS[69,91,92]. ECs transfected with dominant negative Rac show an inhibited orientation of actin fibers with the direction of flow as well as reduced migration speed[69]. It has been suggested that FAK signaling pathways may be responsible for the

mechanotranduction in shear stress-triggered EC migration in that a FAK inhibitor AG213 delays the wound healing process and dominant negative FAK construct overexpression decreases the EC motility[93,94]. Urbich et al. have also illustrated that LS facilities EC migration via integrin-ECM binding[95]. Taken together, shear stress-mediated EC migration can be mechanosensed by focal adhesion complex and is tightly associated with Rac, which prominently regulates the orientation of cytoskeletal fibers with the direction of flow.

Endothelial permeability

The continuous endothelium in the arterial tree serves as a semi-permeable barrier that regulates the transport of macromolecules. Hydrophobic substances such as hormones, fatty acids, etc. are bound to albumins for proper delivery across the endothelium barrier[96]. Liquid and protein transport across the endothelium barrier is mainly mediated by the paracellular-junctional and transcellular-vesicular pathways[97]. Endothelial permeability is regarded as one key determinant of endothelial function/dysfunction. Increased endothelial permeability has been implicated in multiple diseases, including atherosclerosis. High endothelial permeability is reflected

by the abnormal accumulation of low-density lipoprotein (LDL) in the intima of arterial segments in specific regions[98,99] where OS is predominant[100], suggesting its correlation with fluid shear stress. *In vivo* uptake of Evans Blue in porcine iliac arteries have illustrated that endothelial permeability inversely correlates with the magnitude of LS[101]. Multiple shear stress-induced signaling molecules have been proposed in the modulation of EC permeability, including NO, cAMP, phosphorylated junctional proteins, etc.. In general, it is the cytoskeletal alteration that leads to increased liquid and protein permeability. Studies on inhibition of eNOS activity have revealed that decreased intracellular NO level increase EC permeability by altering actin cytoskeleton[102] and enhancing thrombin expression[103]. cAMP has also been suggested to play a role in LS-induced lowering of EC permeability by activating PKA signaling pathway[104]. Focal adhesive molecule occludin can be phosphorylated by shear stress, which may stabilize occludin to tight junction and maintain the low EC permeability under LS[105]. These findings shed light on the molecular mechanisms of fluid shear stress-induced modulation of EC permeability.

EC alignment

Shear stress has been well-documented as a driving force in EC elongation and alignment with the direction of flow[106,107]. ECs in static culture are in a polygonal cobblestone-like shape whereas those under LS are spindle-shaped and aligned with the direction of flow[108](Figure 3). Notably, cessation of flow can reverse the spindle-shaped ECs back to polygonal over time[109]. This shear stress-induced morphological changes are dependent on the exposure time and the magnitude of shear stress[110]. Galbraith et al. have investigated the elongation and orientation in the direction of flow and hypothesized 3 phases for EC morphological changes under LS. In the first 3 hours, ECs undergo a cytoskeletal change with an increased number of stress fibers and redistribute the adhesion sites to the edge of cells. In the next 3-hour window, cell movement is observed as an outcome of the loss of peripheral bands and the nucleus is relocated to the upstream side, After 12 hours, more ECs are elongated and oriented with the direction of flow with enough thick stress fibers and microfilaments to adapt to the frictional force[111]. Shear stress-induced cytoskeletal changes are mediated by multiple signaling pathways, including intracellular calcium release,

extracellular calcium influx, inositol trisphosphate and diacylglycerol increase[112-114]. In addition, small GTPases RhoA and Rac1 have been indicated to contribute to the adaptation of endothelial cytoskeleton to LS[69].

Vascular tone regulation

In addition to the counteraction between sympathetic and parasympathetic nerves in regulating the vascular tone, ECs lining along the luminal surface of the vasculature synthesize, store and release a wide range of vasoactive molecules, including NO, endothelin-1 (ET-1), prostaglandin I_2 (PGI_2), etc. in response to the biomechanical stimulation[115]. These vasoactive molecules are implicated to play a key role in the vascular physiology and pathophysiology[116-118]. NO is produced by phosphorylated eNOS in

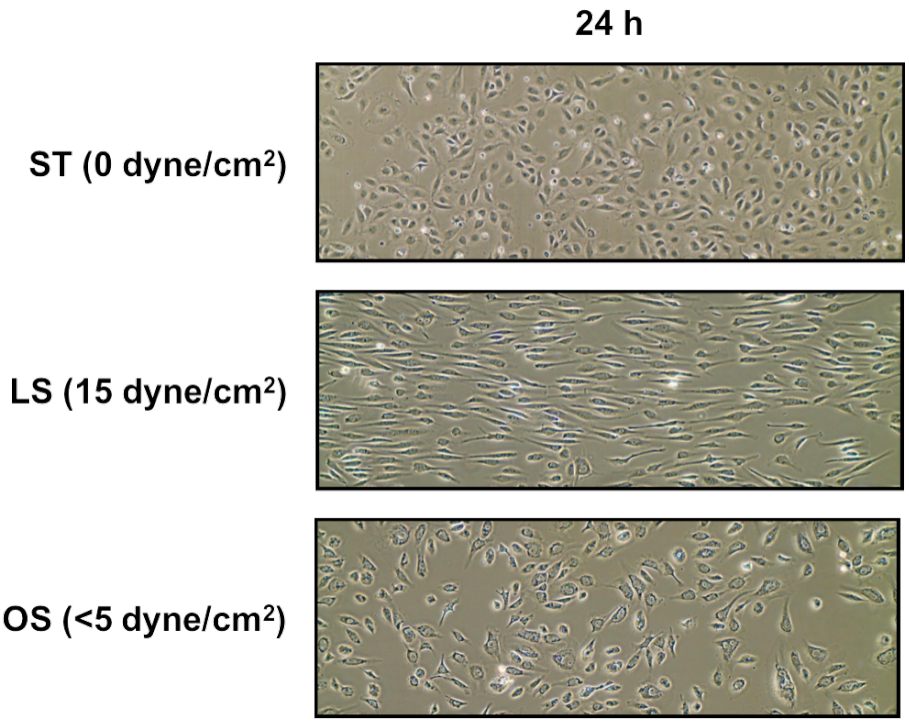

Figure 3. Representative light microscopic images of HUVECs under different shear stress conditions for 24 hours. (magnification = 10X)

ECs in response to LS[71]. The elevated NO level activates guanylate cyclase to increase cyclic guanosine monophosphate (cGMP) in vascular smooth muscle cell (VSMC) for vasorelaxation[119]. In contrast, ET-1 is a well-known EC-derived vasoconstrictor[120]. Interestingly, ET-1 can also be regulated by fluid shear stress. Kuchan et al. have reported that both long-term exposure to low shear stress (1.8 dyne/cm^2) and short-term exposure to physiological LS (<1h) stimulate the release of ET-1 in cultured EC. This release of ET-1 may be mediated by PKC signaling pathways[76] and itself acts

as an agonist of L-type calcium channels to trigger the vasoconstrictive effect[121]. PGI_2 is a potent vasodilator. Early studies have shown that LS significantly increases PGI_2 production, which peaks at the onset of flow as well as at 2 hour and beyond[122]. The onset peak of PGI_2 production may be due to the calcium-dependent phospholipase cytosolic phospholipase A_2 activation[123]. Okahara et al. later have demonstrated sustained PGI_2 production under long-term LS may be attributed to increased expression of cyclooxygenases and PGI synthase[124].

Shear stress in the process of atherosclerosis

Hemodynamic forces are actively involved in the pathogenesis of cardiovascular diseases, such as aneurysm, aortic dissection, aortic valve calcification and atherosclerosis[125-127]. Atherosclerosis is characterized by the deposition of excessive lipids, the infiltration of inflammatory cells, the aberrant proliferation and apoptosis of ECs and VSMCs[128]. The pathogenesis of atherosclerosis is a multifactorial process with hundreds of stimuli and factors involved, both locally and systematically. It develops in the intimal layer of the vascular wall with preference in areas of lesser curvatures and arterial bifurcations in the arterial tree[129]. This heterogeneity

of distribution is believed to be associated with fluid shear stress, which predominantly contributes to the endothelial biology[130]. In the 1970s, there are two opposite hypotheses regarding the effect of shear stress on the unique distribution pattern of atherosclerosis. One suggested that high shear stress (400 dyne/cm^2) rubbed the endothelial layer leading to cell injury at focal areas, which may initiate atherosclerosis[131]. The other favored low shear stress as a biomechanical catalyst in the process of atherogenesis[132]. With decades of efforts, people now realize that low and oscillatory shear stress (OS) derived from disturbed flow predisposes the vascular intima to atherosclerosis[129,133-135]. Cheng et al. have investigated the correlation between shear stress pattern and the size of atherosclerotic lesion as well as its vulnerability. They employed a perivascular shear stress modifier to induce different shear stresses in one carotid artery of ApoE$^{-/-}$ mice fed with western diet. Intriguingly, segments under lowered shear stress were illustrated with a larger red oil o staining area and less collagen production whereas plaques in those under OS were smaller but more stable. In contrast, the segment under elevated LS were free of atherosclerotic lesions. Taken together, low shear stress predisposes vascular wall to larger vulnerable lesions whereas OS induces stable ones. Arterial segments under high-magnitude LS is free of lesions and evidenced as atheroprotective[136].

Mechanistically, OS have been proposed to attenuate NO-mediated atheroprotection by reducing eNOS expression[137]. The bioavailability of NO is the key to normal vascular tone with strong anti-inflammatory, anti-apoptotic, anti-thrombotic properties[138]. The reduction of NO and other junction proteins such as connexins and VE-cadherin increases the EC permeability allowing pro-inflammatory cells to move inward into the intima[102,103,139,140]. Atherosclerosis is recognized as a chronic inflammatory disease, the initiation of which involves leukocytes recruitment. The recruited cells, including monocytes and macrophages, adhere to the endothelium for subsequent rolling and migration into the intimal layer[141] and become foam cells[85,142]. This process is mediated by a wide range of proinflammatory molecules, such as chemokines, adhesion molecules and oxidized lipoproteins. LS is recognized as a potent inhibitor of vascular cell adhesion molecule 1(VCAM-1) and E-selectin upon tissue necrosis factor-α (TNF-α) stimulation in ECs[143]. By contrast, OS potentiates monocyte adhesion by up-regulating adhesion molecules[144]. In addition, OS has been shown to increase nuclear factor κB (NF-κB) expression in ECs *in vitro*[145]. Other pro-inflammatory signaling pathways such as JNK[146] can be regulated by OS as well, weighing OS as a crucial pro-atherogenic factor. The activation and sustainment of inflammation accelerates endothelial dysfunction,

contributing to the development of atherosclerosis. Another characteristic of atherosclerosis is the massive deposition of lipids. It seems to correlate with the cholesterol level in the blood while it is not uniformly accumulated in the arterial tree indicating that there must be another determinant responsible for the unique pattern. Animal and computational studies provide evidence linking shear stress patterns to plaque distribution[136,147,148]. OS has been implicated to increase the EC permeability to lipid protein LDL[99,149] and upregulate LDL receptor expression[150]. This OS-induced pro-atherogenic effect along with high blood cholesterol level promotes lesion formation and growth.

Summary

A large amount of efforts has been made to investigate the molecular mechanisms of OS-induced atherogenesis. From mechanosensing to transcriptional regulation, from in vitro flow simulation system to in vivo animal models, advances in the knowledge of OS-induced endothelial dysfunction are progressing rapidly. It is clear that OS determines the distribution of atherosclerosis in the arterial tree[151]. In addition, exercise-induced vasoprotective effects are correlated with increased LS[152,153]. However, the underlying mechanisms remain to be addressed. Shear stress-

sensitive genes are implicated to be heavily involved in the complex network of signal sensors, messengers, regulators, and effectors, interactions of which are believed to be the key to endothelial function. Thus, we hypothesize that there are novel shear stress-sensitive genes that are involved in the process of atherosclerosis, elucidating which may help to understand the underlying mechanisms of atherogenesis. To address these biological questions, I performed RNA sequencing to profile the whole transcriptome of primary human coronary artery ECs under LS, OS and static culture condition (ST) to understand the transcriptomic differences in ECs under different types of shear stress.

CHAPTER II

Effects of shear stress on the whole transcriptome in HCAECs

Previously published as Qiao C *et al.,* Deep transcriptomic profiling reveals the similarity between endothelial cells cultured under static and oscillatory shear stress conditions. Physiological Genomics. 2016; DOI: 10.1152/physiolgenomics.00025.

This chapter contains collaborative work performed with Dr. Inhwan Jang from the laboratory of Dr. Hanjoong Jo at Georgia Institute of Technology and Emory University and Dr. Fan Meng at the University of Michigan. Dr. Inhwan Jang performed the shear stress experiments and Dr. Fan Meng analyzed the bioinformatic data. I performed the remainder of this work.

Introduction

ECs are constantly exposed to hemodynamic shear stress, which is the frictional force generated by blood flow. Alterations in the magnitude and direction of shear stress predominantly determine the mechanotransduction-

mediated endothelial functional phenotype[154,155]. High laminar shear stress (LS, ≥15 dyne/cm^2) presented in straight unbranched vascular lumen is commonly denoted as athero-protective shear stress. LS maintains the endothelial "quiescent" tone[10] by inhibiting adhesion molecules expression[143,156], suppressing the potent vasoconstrictor ET-1[157], inducing the proliferation inhibitor p21[80], as well as preventing endothelial cell apoptosis[158] thereby maintaining vascular and endothelial homeostasis. ECs under LS exert strong vasoprotective effects through increased NO production by eNOS phosphorylation[159,160] in a Krüppel-like factor 2 (KLF2)-dependent manner[161,162]. By contrast, low or oscillatory shear stress (OS) (0~5 dyne/cm^2) found in areas of disturbed flow, such as arterial bifurcations and lesser curvature of aortic arch, is well-documented as a pro-atherogenic force[5,163]. Animal studies focusing on the aorta[134,164] and carotid arteries[165] provide solid evidence that OS predisposes the vascular intima to atherogenesis. Human ultrasonographic imaging further demonstrates an inverse correlation between carotid artery thickness and local shear stress magnitude[166]. The critical role of shear stress in the geometrical distribution of atherosclerosis has led to intense research interest in determining the underlying pathogenic mechanisms[129].

Efforts have been made to survey the changes in shear force-mediated gene expression in ECs using a DNA microarray approach. These studies have shown distinctive gene expression patterns between ECs under LS and OS conditions[167,168], LS and static (ST) conditions[161,169], or LS, OS and ST conditions together[170]. The results indicate a strong phenotypic plasticity of ECs in response to shear stress. However, microarray studies have only identified a small portion of gene expression changes in response to different types of shear stress, which is unlikely to provide a complete profile of the full transcriptome since microarray probes or probe sets are mainly based on previously mapped genes[171]. In addition, microarrays fail to detect novel unannotated transcripts and in particular, a large number of non-coding RNAs (ncRNAs)[172] within a transcriptomic pool.

While approximately 80% of the mammalian genome is actively transcribed, protein-coding transcripts only account for about 2%[173]. NcRNAs with little potential for translation were dismissed as junk RNA in the 1970s[174]. Today, it is clear that ncRNAs are responsible for critical biological functions as well. Emerging evidence shows that ncRNAs including microRNAs[175] and long ncRNAs (lncRNAs) [176,177] are key players in the regulation of the transcription process. LncRNAs are a group of RNAs that are longer than 200 nucleotides

and are proposed in the development of multiple diseases[178,179]. Studying lncRNAs' function and expression may help to elucidate the molecular mechanisms of the development of atherosclerosis.

Given that the endothelial layer is constantly exposed to hemodynamic forces once the cardiovascular system develops during embryogenesis[180], the ST condition is the least reminiscent of the hemodynamic milieu *in vivo*. Despite this, a tremendous amount of EC research has been conducted under ST conditions. The results of this work may not be translatable to subsequent *in vivo* studies due to the missing biomechanical milieu[181]. Here, I use RNA sequencing (RNA-seq)[182] to profile the whole transcriptome of primary human coronary arterial ECs (HCAECs) under LS (15 dyne/cm^2), OS (0~5 dyne/cm^2), and ST conditions. My goal was to survey the transcriptomic difference under different shear stress conditions to test the hypothesis that there are novel shear stress-sensitive genes that are involved in the process of atherosclerosis, elucidating which may be the key to understanding the underlying mechanisms of atherogenesis.

Materials and methods

ECs culture

Human coronary artery endothelial cells (HCAECs) were obtained from Cell Applications (San Diego, CA) at passage 2 and cultured in MesoEndo Cell Growth Medium or Endothelial Cell Basal Medium (Cell Applications). The Growth Medium contains 5% fetal bovine serum, 10 ng/mL human epidermal growth factor, and 6 ng/mL basic fibroblast growth factor. Cells were incubated at 37 °C in a standard cell culture incubator. HCAECs were used at passage 6 in the following studies.

Shear stress studies

A detailed protocol has been described previously[183]. Briefly, HCAECs monolayers at confluence in 100-mm tissue culture dishes were exposed to arterial levels of unidirectional LS (15 dyne/cm^2), bidirectional OS at 1 Hz cycle (0~5 dyne/cm^2) by rotating a Teflon cone (0.5° cone angle) with a stepping motor (Servo Motor) and a computer program (DC Motor Company, GA), and static culture condition for 24 hours (n=4 for each conditions).

RNA isolation and RNA-seq library preparation

After exposed to LS, OS and ST for 24 hours, ECs were harvested by scraping, and RNA was isolated and purified using RNeasy mini kit and subjected to on-column RNase-free DNase treatment according to product protocol (Qiagen, CA). Total RNA from 12 samples was then assessed for quality using the BioAnalyzer (Agilent, CA). Double-stranded cDNA was generated from 100 to 150 ng of total RNA using selective priming and prepared for the final library. Samples with RNA Integrity Numbers of 8 or greater were prepared using the EnCore Complete RNA Seq Library System (NuGen, CA). Final libraries were checked for quality as well as quantity by the BioAnalyzer DNA 1000 (Agilent, Santa Clara, CA). Quantitative PCR (qPCR) for was performed to quantify the library using a KAPA kit (Kapa Biosystems, MA) for Illumina sequencing platforms. Twelve samples were then clustered on the cBot and sequenced on a 50-cycle single end on a HiSeq2000 (Illumina, CA) to generate 50 bp paired-end reads, using TruSeq SBS v3 reagents (Illumina, WI) according to manufacturer's protocols.

RNA-seq data analysis and quantitative PCR

RNA-seq fastq files were aligned to the human genome primary assembly (GRCh38) using the Subread package[184]. Read counts on each gene were determined by featureCounts function in the Subread package using GeneCode human GTF file version 23(http://www.gencodegenes.org/). Differential expression analysis between different cell culture treatments were performed using the limma package with the voom transformation[185]. P values were adjusted by default Benjamini-Hochberg procedure. We require at least 4 samples have normalized read counts of >= 1 rpm (one count per million aligned reads) to include a gene in the differential expression analysis and other downstream analyses.

Collected RNA was reverse-transcribed into cDNA pool with SuperScript III RT-PCR kit (Invitrogen, CA). Target RNAs expression was determined by a qPCR System (Bio-Rad, CA) using iQ SYBR Green Supermix (Bio-Rad). The gene expression was normalized against the internal control, 18S rRNA. All the primer sequences are shown in Table 2.

Table 2: Sequence of primers used for qPCR quantification

Gene	Species	Forward	Reverse
KLF2	HUMAN	5'-AGCCTTCGGTCTCTTCGAC-3'	5'-GCGAACTCTTGGTGTAGGTCTT-3'
NOS3	HUMAN	5'-ATGGATGAGTATGACGTGGTGT-3'	5'-ATGCTGTTGAAGCGGATCTTAT-3'
ID1	HUMAN	5'-GCAGGTAAACGTGCTGCTCTAC-3'	5'-AGTTCAGCTCCAACTGAAGGTC-3'
KLF11	HUMAN	5'-CTGTCTCTGACTCTGGGGATGT-3'	5'-TGGAATCTGTTACTTGGGGAGA-3'
LMO7	HUMAN	5'-AAGACTGCGTTACCCTTCAATC-3'	5'-TGGACTTACTCCCATTCTCACC-3'
TEK	HUMAN	5'-CCCTCCTCCAAGAGGTCTAAAT-3'	5'-GTACTGCTCCCTGGGATGTAAG-3'
HYAL2	HUMAN	5'-ACTGGCAGGACAAAGATGTGTA-3'	5'-GAAAGAGGTAGAAGCCCCAGAG-3'
SERPINE2	HUMAN	5'-AATCCTATCAAGTGCCAATGCT-3'	5'-CTGTCTATGGTCTTGGTGCTGA-3'
C10orf10	HUMAN	5'-ATAGACAGATGGACAGCAGCAA-3'	5'-GGAGGTGCGAGTAGAGTGTTCT-3'
CXCR4	HUMAN	5'-AAGGCAGTCCATGTCATCTACA-3'	5'-GCAAAGATGAAGTCGGGAATAG-3'
ANGPT2	HUMAN	5'-AAACGCGGAAGTTAACTGATGT-3'	5'-TGATGTGCTTGTCTTCCATAGC-3'
FABP4	HUMAN	5'-AGAAGTAGGAGTGGGCTTTGC-3'	5'-CCCATCTAAGGTTATGGTGCTC-3'
LXN	HUMAN	5'-GGTGAACTGCACAGCTGAAGTA-3'	5'-GAGCGTCATTTCTGGAGATACA-3'
EFNA1	HUMAN	5'-ACTGTACCTGGTGGAGCATGAG-3'	5'-GCCTGAGGACTGTGAGAGATGT-3'
CCL14	HUMAN	5'-ACCAAGACTGAATCCTCCTCAC-3'	5'- CCCTTTTGGTGATGAAGACAAT-3'
VCAM1	HUMAN	5'-AAAAGCGGAGACAGGAGACA-3'	5'-AGCACGAGAAGCTCAGGAGA-3'
18S	HUMAN	5'-GGAAGGGCACCACCAGGAGT-3'	5'-TGCAGCCCCGGACATCTAAG-3'

Cell Extracts and Western Blotting

Whole cells were lysed using Pierce RIPA buffer (Thermo Scientific, MA) supplemented with a protease inhibitor cocktail (Roche Applied Science, IN). Briefly, 30 µg of protein sample were loaded per lane on a SDS-PAGE gel, separated by gel electrophoresis, and transferred to a 0.2 µm nitrocellulose membrane (Bio-Rad). Membranes were blocked in 5% nonfat milk in Tris-HCl buffer saline with tween (TBST) and incubated with anti-β-actin, anti-ID1, anti-FABP4, anti-EFNA1, anti-LMO7, anti-KLF2 (Santa Cruz Biotechnology, CA), anti-HYAL2, anti-CCL14 (ThermoFisher Scientific, MA), anti-NOS3 (Cell Signaling Technology, MA), anti-SERPINE2, anti-LXN, anti-ANGPT2, anti-TEK (R&D systems, MN),

or anti-KLF11 (Novus Biologicals, CO) antibodies at 4 ˚C overnight. After TBST washing, membranes were incubated with a diluted (1: 10,000) IRDye-conjugated secondary antibody (Li-Cor Biotechnology, NE) for 1 hour at room temperature. Immunoblots were scanned and the intensity of the protein bands was quantified using Image Studio software (Li-Cor).

Statistical Analysis

Statistical analyses among 3 groups were performed by one-way ANOVA with Bonferroni post hoc test. A $p < 0.05$ was considered statistically significant. Data are presented as means ± SEM.

Results

Shear stress substantially impacts on endothelial transcriptome

Among 16,313 genes with at least one read count per million (>=1 rpm), more than half of the genes in ECs under OS or ST condition were differentially expressed compared to those under LS (8,177 for OS vs LS and 9,369 for ST vs LS) at the FDR ≤ 0.05 threshold. On the other hand, only 1,618 of the genes were differentially expressed between ECs under ST and OS at the same threshold. All genes were

categorized into 5 groups: protein-coding genes, pseudogenes, antisense genes, genes for long intervening ncRNAs (lincRNAs), and others (Figure 4).

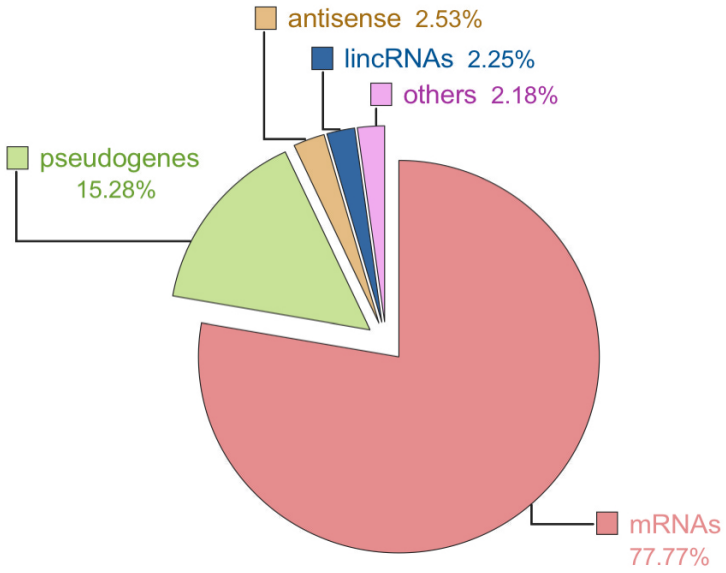

Figure 4. A pie chart showing the distribution of all detected transcripts as messenger RNAs (mRNAs), pseudogenes, antisense, long intervening non-coding RNAs (lincRNAs) and other transcripts.

For quantitative real-time PCR (qPCR) confirmation, we selected a group of well-known shear-sensitive genes, including KLF2, eNOS, hyaluronoglucosaminidase 2 (HYAL2), C-X-C chemokine receptor type 4 (CXCR4), angiopoietin-2 (ANGPT2), fatty acid binding protein 4 (FABP4), vascular cell adhesion molecule 1 (VCAM1), inhibitor of DNA binding 1 (ID1) and some novel shear-sensitive genes, including KLF11, LIM domain 7 (LMO7), TEK tyrosine kinase (TEK), serpin

peptidase inhibitor member 2 (SERPINE2), chromosome 10 open reading frame 10 (C10orf10), latexin (LXN), Ephrin-A1 (EFNA1) and chemokine (C-C motif) ligand 14 (CCL14) for qPCR analysis. The qPCR data showed a comparable fold change of gene expression levels in ECs under ST (Figure 5A) and OS (Figure 5B) in comparison to LS.

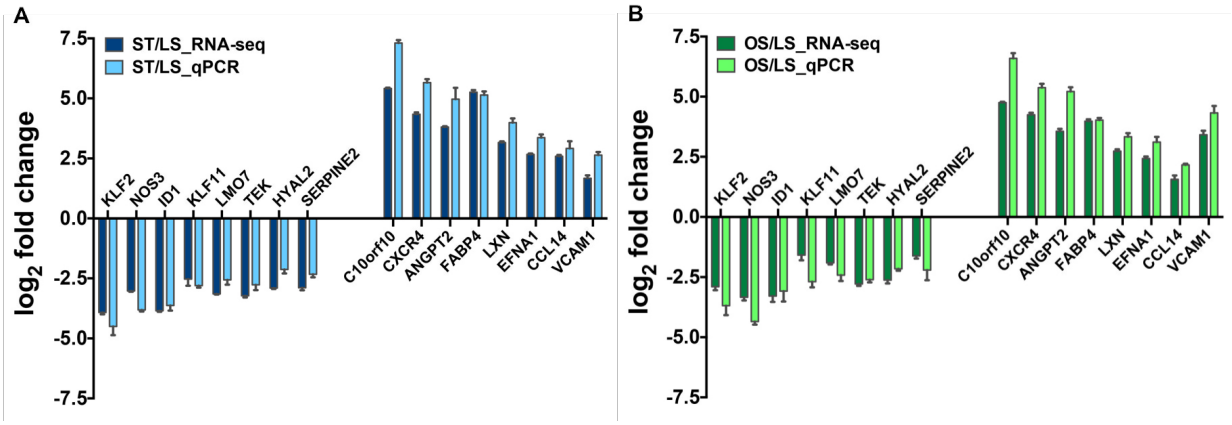

Figure 5. qPCR confirmation of representative genes detected by RNA-seq under ST **(A)** and OS **(B)** including Krüppel-like factor 2 (KLF2), nitric oxide synthase 3 (NOS3), inhibitor of DNA binding 1 (ID1), KLF11, LIM domain 7 (LMO7), TEK tyrosine kinase (TEK), hyaluronoglucosaminidase 2 (HYAL2), serpin peptidase inhibitor member 2 (SERPINE2), chromosome 10 open reading frame 10 (C10orf10), C-X-C chemokine receptor type 4 (CXCR4), angiopoietin-2 (ANGPT2), fatty acid binding protein 4 (FABP4), latexin (LXN), Ephrin-A1 (EFNA1), chemokine (C-C motif) ligand 14 (CCL14), vascular cell adhesion molecule 1 (VCAM1). (N=4, respectively)

Transcriptome analysis reveals similarities between ECs under OS and ST conditions

One salient observation from the RNA-seq data is the high similarity of gene expression profiles for ECs under OS and ST conditions. For

differentially expressed genes listed from OS vs LS and ST vs LS, a total of 7,220 genes (88.3% in OS vs. LS; 77.1% in ST vs. LS) showed overlapping expression patterns. We further examined these genes according to their gene types. Numbers of genes that were differentially up- or down-regulated in ECs under ST and OS are shown in proportional Venn diagrams for each group (Figure 6A-E). A large proportion of genes in each category were overlapped under OS and ST. qPCR comparisons of the same genes in Figure 1B and 1C confirmed the gene expression resemblance in ECs under ST and OS conditions (Figure 6F).

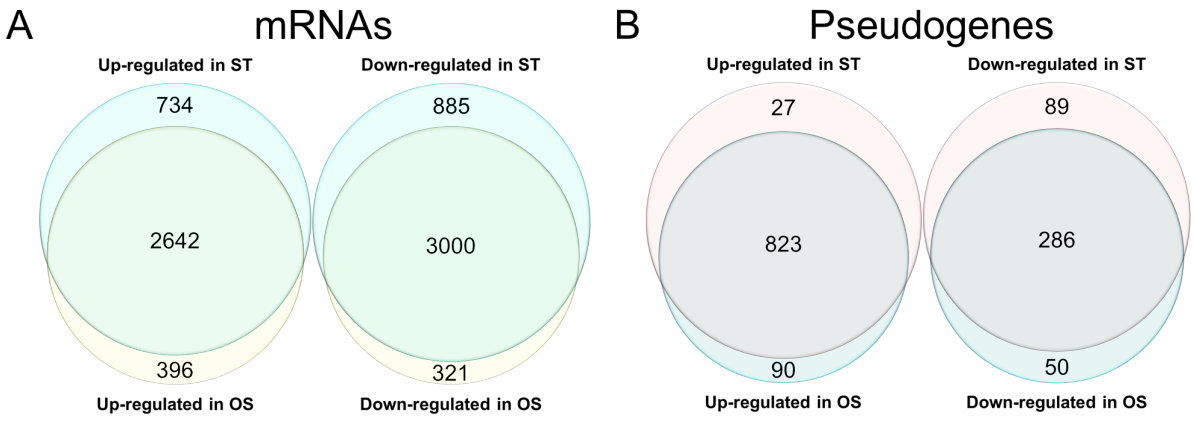

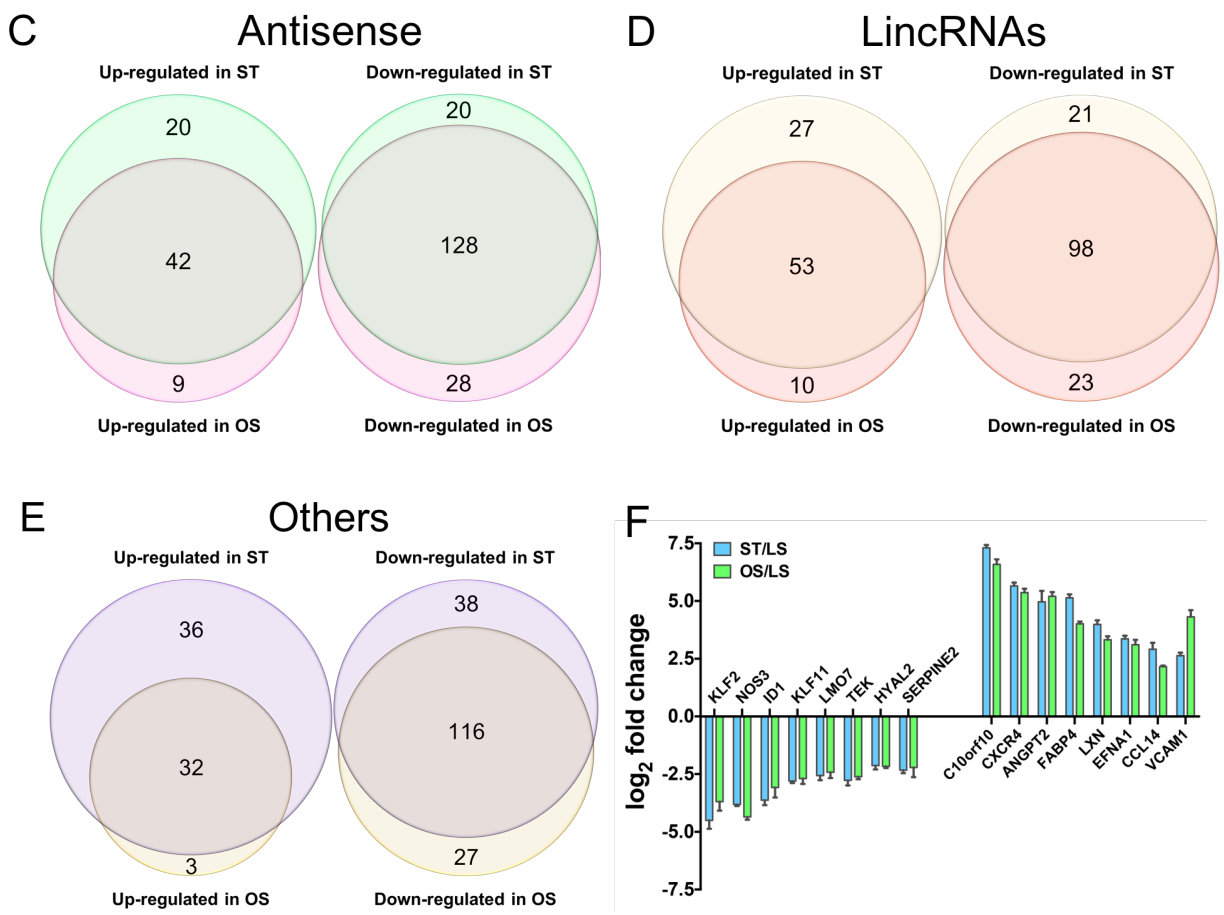

Figure 6. Proportional Venn diagrams of differentially expressed transcripts under ST and OS. Numbers of mRNAs **(A)**, pseudogenes **(B)**, antisense transcripts **(C)**, lincRNAs **(D)** and others **(E)** that were differentially expressed in ECs under OS and ST. The overlap of the two circles represents common transcripts under OS and ST. Comparison of qPCR results under ST and OS **(F)**. (N=4, respectively)

We also examined gene expression profile at individual sample level. Hierarchical clustering analysis demonstrated a strong similarity between OS and ST samples (Figure 7A), which was further confirmed by a pairwise similarity heat map (Figure 7B). In principal component analysis, ST and OS samples were completely separated

from LS samples and the shorter distance between ST and OS samples indicated the higher similarity between ST and OS (Figure 7C).

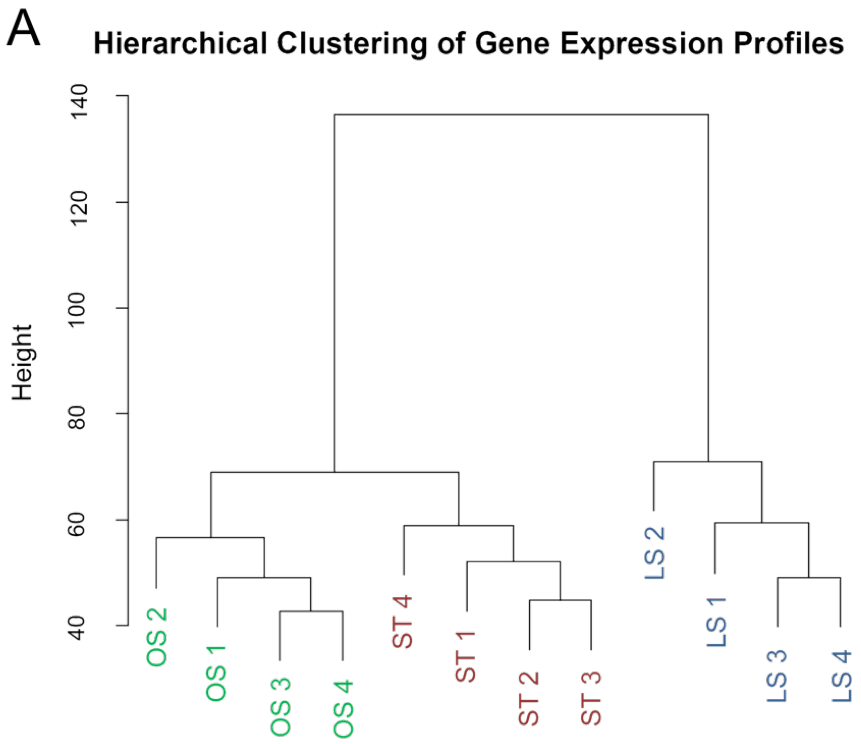

B

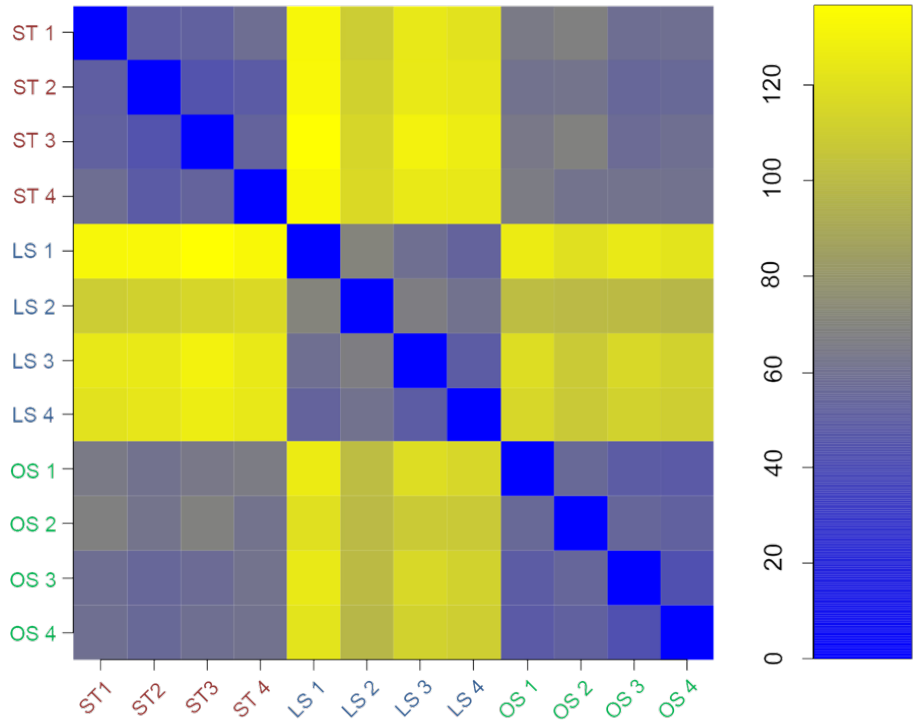
Gene Expression Profile Distance
ST 1
ST 2
ST 3
ST 4
LS 1
LS 2
LS 3
LS 4
OS 1
OS 2
OS 3
OS 4
ST1
ST2
ST3
ST 4
LS 1
LS 2
LS 3
LS 4
OS 1
OS 2
OS 3
OS 4
0
20
40
60
80
100
120

C

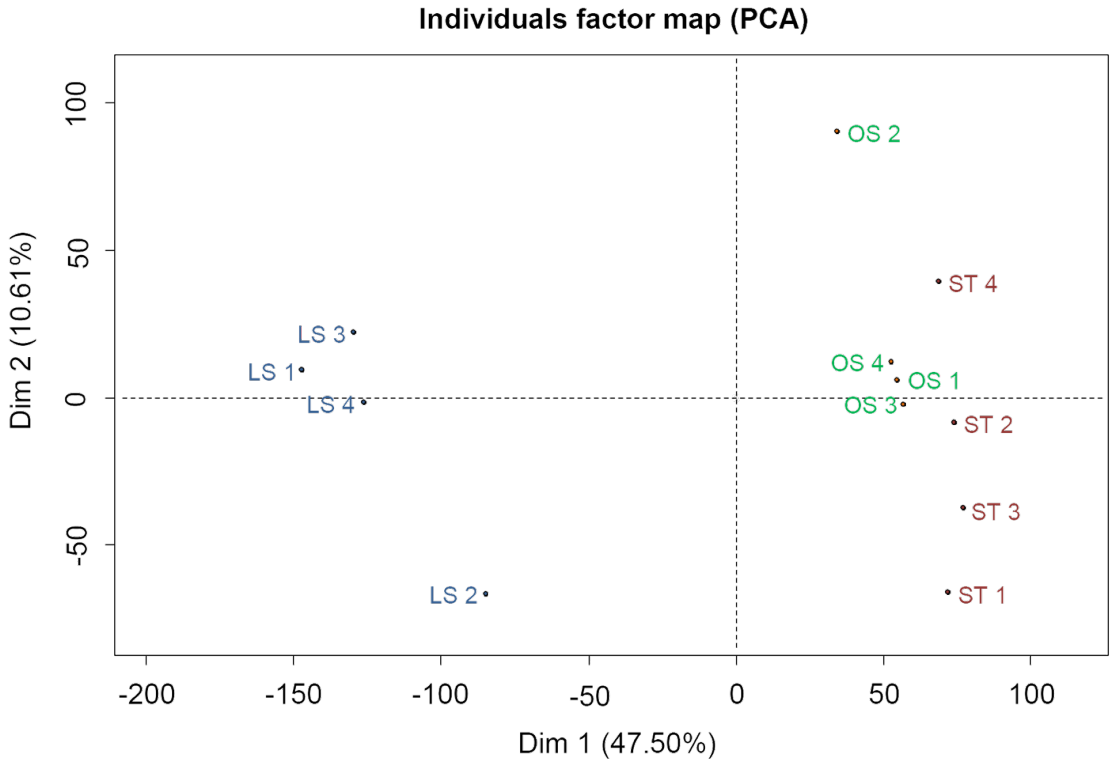
Individuals factor map (PCA)
Dim 2 (10.61%)
100
50
0
-50
OS 2
ST 4
LS 3
OS 4
LS 1
OS 1
LS 4
OS 3
ST 2
ST 3
LS 2
ST 1
-200
-150
-100
-50
0
50
100
Dim 1 (47.50%)

Figure 7. Gene expression profile shows a strong similarity between endothelial transcriptome under ST and OS. **(A)** Hierarchical clustering profile reveals detailed relationships between all samples under ST, OS and LS. The vertical distance reflects the similarity between samples. **(B)** Heat map of all 12 samples using Euclidean distance as a measure parameter. **(C)** Principle component analysis of gene expression profiles from each sample under ST, OS and LS demonstrates the major components (Dim 1 & 2) of the variance to separate samples. Dim 1 and Dim 2 accounts for 47.5% and 10.61% of the total variance, respectively.

Biological evidence supports the similarities beteween ECs under OS and ST

In addition to the comparable expression of these representative genes at the transcript level (Figure 6F), we sought to exam their protein levels in ECs under ST, OS and LS conditions. We performed immunoblots for KLF2, NOS3, ID1, KLF11, LMO7, TEK, HYAL2, SERPINE2, ANGPT2, LXN, FABP4, EFNA1 and CCL14 under ST, OS and LS conditions (Figure 8). These representative Western blots contain 3 sets of protein extracts from 3 independent experiments under ST, OS and LS conditions (Figure 8A). Expression levels under ST and OS conditions showed a significantly up- or down-regulation in comparison to those under LS condition. Notably, there is no significance at the protein level of these genes in ECs under OS and ST conditions.

A

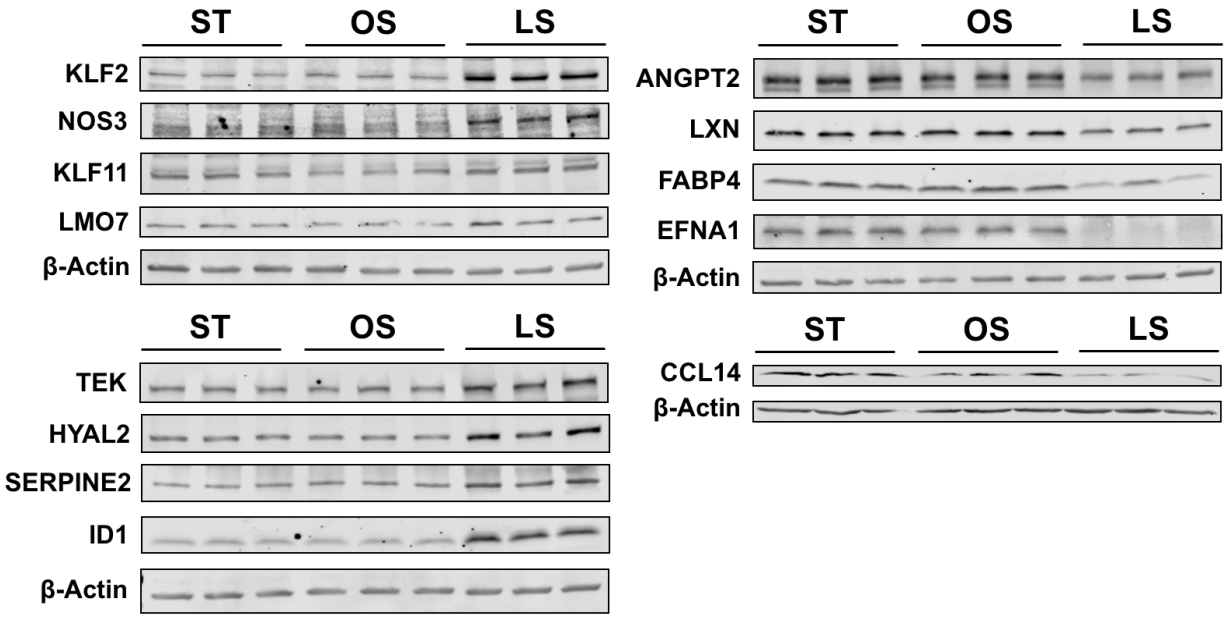
ST
OS
LS
KLF2
NOS3
KLF11
LMO7
β-Actin
ANGPT2
LXN
FABP4
EFNA1
TEK
HYAL2
SERPINE2
ID1
CCL14

B

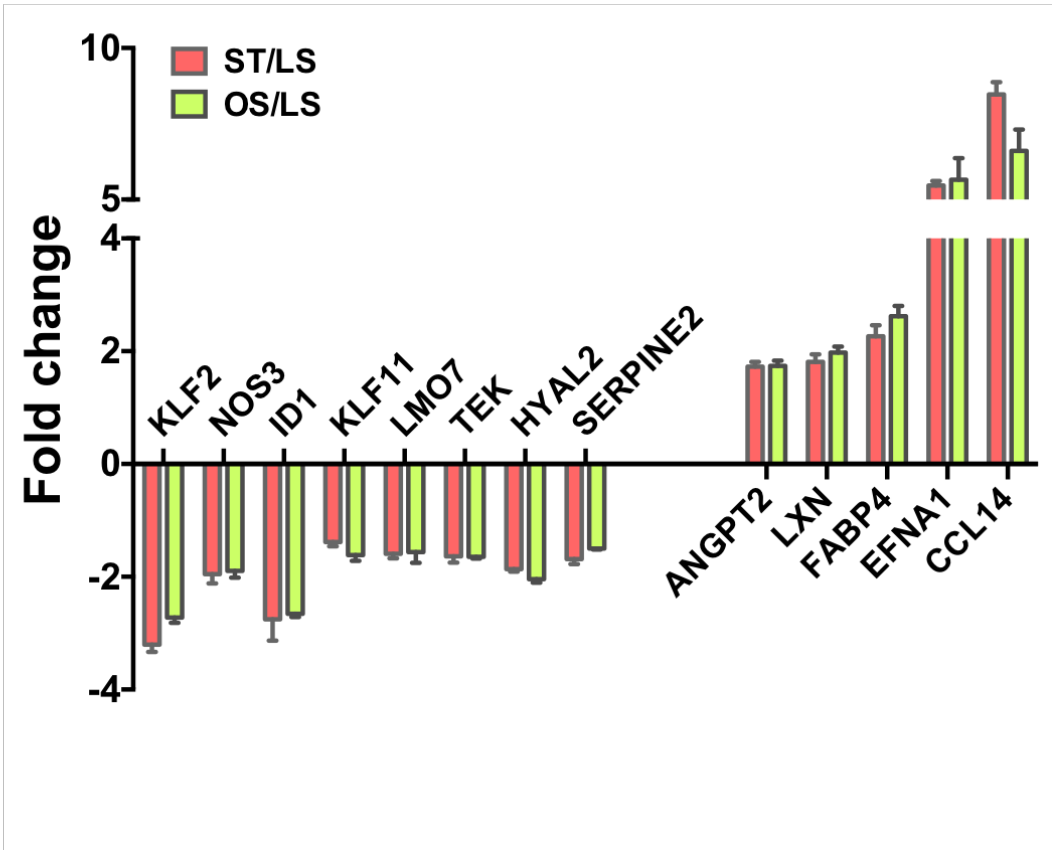
ST/LS
OS/LS
Fold change
10
5
4
2
0
-2
-4
KLF2
NOS3
ID1
KLF11
LMO7
TEK
HYAL2
SERPINE2
ANGPT2
LXN
FABP4
EFNA1
CCL14

Figure 8. Protein expression level of representative shear-sensitive genes in ECs under ST, OS and LS conditions**. (A)** Representative Western blots show the protein level of KLF2, NOS3, ID1, KLF11, LMO7, TEK, HYAL2, SERPINE2, ANGPT2, LXN, FABP4, EFNA1 and CCL14 (β-actin as loading control) in HCAECs under ST, OS and LS conditions for 24 hours. **(B)** The band intensity was quantitatively analyzed and normalized against the loading control, β-actin. Data are from 3 independent experiments and presented as mean ± SEM.

Discussion

Here, I profiled whole transcriptome of primary HCAECs using RNA-seq under the shear stress conditions of LS, OS and ST. The data demonstrate that the endothelial transcriptomic profile under LS condition profoundly differs from those under either ST or OS conditions. Intriguingly, high transcriptomic similarities were found in ECs under ST and OS conditions. Chen *et al.* suggested that results obtained under LS conditions should be the reference given the biomechanical milieu *in vivo*, thus the absence of shear stress may be a pathological situation, suggesting that ECs under ST may deviate from normal[169]. García-Cardeña *et al.* first described that there were much less differentially expressed genes in OS vs. ST than LS vs. ST conditions[170]. However, due to limitations of the DNA microarray method, it was unlikely to distinguish the whole endothelial transcriptome under different shear stress conditions. Based on our RNA-seq data, we found that 52.8% of differentially expressed genes in HCAECs under ST vs. OS

conditions were in the same change direction compared to LS condition. For example, there was a 2.5-fold up-regulation of VCAM1 expression in ST vs LS conditions and an approximately 4-fold up-regulation in OS vs LS conditions, which accounts for a 1.5-fold difference between ST and OS conditions (Figure 6F). Functional studies have demonstrated that there is greater human monocyte binding to ECs under either OS or ST in comparison to LS condition[156,186]. Notably, there is no significant difference in the number of binding monocytes to ECs under ST and OS conditions[186], indicating that ECs under ST may be more pathologically relevant. Unfortunately, due to a lack of good antibodies to assess endogenous protein levels of C10orf10, CXCR4 and VCAM1, I was not able to immunoblot them from cell extracts to determine changes under ST, OS and LS conditions.

It is widely recognized that ECs in culture are different from those *in vivo*[187]. The absence of hormonal and biomechanical stimuli are the two major forces[11]. While the hormonal environment can be compensated for by introducing growth factors into the culture medium, the lack of biomechanical stimulation makes ECs in culture phenotypically different from those *in vivo*[111,188]. I employed ECs at the same passage for the shear stress

experiments to minimize the artifacts from environment (e.g. culture condition) and preparation, however, it took several propagations to obtain enough HCAECs for all the shear stress experiments. It is likely that HCAECs may undergo culture-induced adaptation during propagation, which may limit the interpretation of this study.

In the present work, we exposed HCAECs to different shear stress conditions for 24 hours. Previous studies have revealed that ECs under prolonged shear stress exhibit a different gene expression profile[161], indicating an important role of temporal factors in shear stress studies. Here, we obtained the endothelial transcriptomic profile at one single time point, which is unlikely to demonstrate the transcript level of transient shear sensitive genes. It will be of great value to survey the dynamic changes of the endothelial transcriptome at different time points in the future.

In terms of individual gene expression levels, the key endothelial transcription factor KLF2, which is one of the master transcription factors in inflammation, thrombosis and vasodilation[160,161], was significantly down-regulated in ECs under ST and OS conditions (Figure 6B and 6C). In addition, the endothelial nitric oxide synthase encoded by NOS3, was dramatically

down-regulated in both conditions as well. Considering its pivotal role in the conversion of L-arginine to nitric oxide, which leads to vascular relaxation and maintains vascular homeostasis, it favors that ECs in culture demonstrate a strong dysfunctional phenotype. LncRNA metastasis-associated lung adenocarcinoma transcript 1 (MALAT1) has emerged as a key regulator in endothelial function. Michalik *et al.* showed a pro-migratory but anti-proliferative endothelial phenotype by silencing MALAT1 *in vitro*[189]. In addition, MALAT1 has been indicated in the control of cell cycle regulators[190]. Our RNA-seq data revealed that MALAT1 is markedly up-regulated by LS whereas there was no significant difference in ECs under both OS and ST conditions (Figure 9). These findings further illustrate the similarity of endothelial transcriptome under OS and ST conditions from a functional lncRNA's perspective.

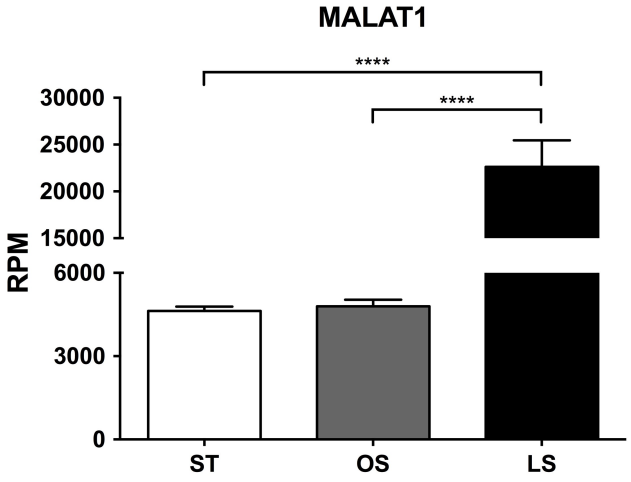

Figure 9. Transcriptome profile reveals the expression of lncRNA MALAT1. The transcript level of MALAT1 detected by RNA-seq are presented as mean ± SEM. ****P<0.0001. (n=4, respectively)

In conclusion, this study focusing on the endothelial transcriptomic profiles under different shear stress conditions provides solid evidence that cultured ECs are significantly different from those under LS condition *in vivo*. The RNA-seq data suggest that the use of ECs under ST condition is unlikely to elucidate relevant endothelial physiology. Given the high similarities of endothelial transcriptomes under OS and ST conditions, it may be helpful to understand the underlying mechanisms of OS-induced endothelial dysfunction from studies in cultured ECs.

CHAPTER III

Laminar shears stress exerts athero-protective effect by inhibiting MIF expression in endothelial cells

This chapter contains collaborative efforts from Dr. Fan Meng at the University of Michigan and Shengdi Li from the Key Lab of Computational Biology at Shanghai Institutes for Biological Sciences. Dr. Fan Meng performed RNA-seq analysis. Shengdi Li performed differential expression analyses. I performed the remainder of this work.

Introduction

Atherosclerosis is the major cause of coronary artery disease as well as stroke, top two killers worldwide[191]. Multiple lines of evidence indicate that endothelial dysfunction is fundamental to the process of atherosclerosis[192]. Once ECs become pathologically activated, pro-inflammatory factors such as TNF-α and interleukin (IL)-1β[193] and adhesive molecules including E-selectin and VCAM1 are up-regulated in ECs for leukocytes recruitment[194]

followed by accumulation of cholesterol-bound lipoprotein[195] and aberrant proliferation of ECs and smooth muscle cells[196], initiating the formation of atherosclerotic lesions. Despite the multifactorial cause of endothelial dysfunction, OS derived from disturbed blood flow contributes significantly to the development of atherosclerosis[5,163]. In contrast to LS in straight vascular lumen, OS is often found in regions of lesser curvatures as well as arterial bifurcation areas[133]. Physiological LS has been shown to increase NO production[159], inhibit adhesion molecules[197] as well as decrease endothelial permeability[101], thus it is recognized as a strong atheroprotective force. Pathological OS compromises endothelial function, resulting in the pathogenesis of atherosclerosis[163]. Human ultrasonographic imaging illustrates that local shear stress magnitude inversely correlates with carotid artery thickness[166]. Animal studies have revealed a causal relationship between OS and atherosclerosis by demonstrating that OS initiates the otherwise atherosclerotic-resistant common carotid arterial intima into atherosclerotic lesion by perivascular constriction[198]. Understanding the molecular mechanisms of biomechanical modulation in endothelial function is a key to the discoveries of potential anti-atherosclerotic drug targets.

Given the revealed atherosclerotic susceptibility in OS-exposed areas, studies have demonstrated that a large variety of pro-inflammatory factors induced by OS are actively involved in the process of atherosclerosis[5]. Macrophage migration inhibitory factor (MIF) is a non-cognate cytokine involved in multiple inflammatory diseases, including atherosclerosis[199]. High MIF levels in atherosclerotic lesions have been documented in animal models[200] as well as human subjects[201]. Multiple lines of evidence have further demonstrated that blockade of MIF reduces the formation of atherosclerotic lesions in animal models[202,203]. In addition to the evidence on the role of MIF in T lymphocytes[204] as well as macrophages[203], which implicates a strong link between MIF and atherosclerosis, the endothelium has been recognized as a significant source of MIF as well[205]. In fact, endothelial MIF has been suggested to play a critical role in response to lipopolysaccharide (LPS)[205] and TNF-α[206] stimulation. Noteworthy, despite the findings that endothelial MIF intimately involves in inflammation, the regulatory mechanisms of MIF expression in the process of atherosclerosis remain to be addressed.

With help from my colleagues, I profiled the whole transcriptome of ECs under different types of shear stress by RNA-sequencing (RNA-seq), the

next generation sequencing that detects novel transcripts such as lncRNAs in addition to annotated protein-coding genes[182,207]. My goal was to survey the undiscovered shear stress sensitive genes that are important in the process of atherosclerosis. I found that MIF can be regulated by shear stress. LS markedly down-regulates MIF expression in ECs whereas OS and ST up-regulates MIF. Thus, I hypothesized that MIF, as a pro-inflammatory cytokine that contributes to the process of atherosclerosis, is shear stress sensitive and its deleterious effect is naturally inhibited by LS *in vivo*, consistent with its anti-atherosclerotic role[208]. This work provides direct evidence to show the great advantage of the next generation sequencing in discovering novel important factors in shear stress-induced regulation of the endothelial transcriptome. In addition, the natural inducer and inhibitor of the pro-inflammatory cytokine MIF lies in the hemodynamic force, which sheds light on the discovery of shear stress sensitive genes in the process of atherosclerosis. The novel shear stress-sensitive transcripts revealed by this work will inform future searches for novel therapeutic drug targets to improve human health.

Materials and Methods

Reagents and antibodies

Primary antibodies against β-actin (sc-1616), KLF2 (sc-28675 X), MIF (sc-20121), VE-cadherin (sc-6458), were purchased from Santa Cruz Biotechnology (Santa Cruz, CA, USA). Primary antibodies against MIF (MAB289-100) for immunocytochemistry was purchased from R & D System (Minneapolis, MN, USA). Secondary Antibodies donkey anti-mouse IgG and donkey anti-goat IgG were purchased from Jackson ImmunoResearch (West Grove, PA, USA). Adenovirus Ad-GFP-h-KLF2, Ad-GFP-U6-hKLF2-shRNA, Ad-GFP-U6-scramble were purchased from Vector Biolabs (Malvern, PA, USA).

Cell culture

Human coronary artery endothelial cells (HCAECs) (Cell Applications, San Diego, CA, USA) were cultured in MesoEndo Cell Growth Medium with 5% CO_2 at 37 °C in a cell culture incubator. Human umbilical vein endothelial cells (HUVECs) (Lonza, Alledale, NJ, USA) were cultured with M199 medium (Invitrogen, Carlsbad, CA, USA) containing 16% fetal bovine serum (FBS), 1 ng/ml recombinant human fibroblast growth factor (Sigma-Aldrich, St. Louis, MO, USA), 90 μg/ml heparin and 20mM HEPES. HCAECs for RNA-sequencing purpose were obtained at passage 2 and used for shear stress

experiments at passage 6 and HUVECs within 4 passages were used in the following experiments. AD-293 (ATCC, VA, USA) cells were cultured in DMEM with 10% FBS.

Shear stress studies and RNA sequencing

A detailed protocol of shear stress experiments for RNA sequencing has been described in material and methods in Chapter II. LS experiments for MIF biology in HUVECs is described here. Briefly, HUVECs at 90% confluence in 80 x 80 mm tissue culture plate were assembled to a flow chamber with silicone gasket and were exposed to 15 dyn/cm^2 unidirectional LS for 24 hours (Figure 10). HUVECs in parallel static cultured condition (ST) were used for control.

RNA-seq analysis

RNA-seq fastq files were aligned to the current version of human genome primary assembly using the Subread program and the GenCode v24 annotation was used for summarizing read counts on each gene. The limma package along with the voom transformation was used for differential expression analysis between different types

of shear stresses. P values were adjusted by default Benjamini-Hochberg procedure. The cutoff requires at least 1 in 4 samples with expression level ≥ 0.1 rpm (one count per aligned million reads) for a gene to be included in the analysis to increase the sensitivity of detecting differentially expressed genes.

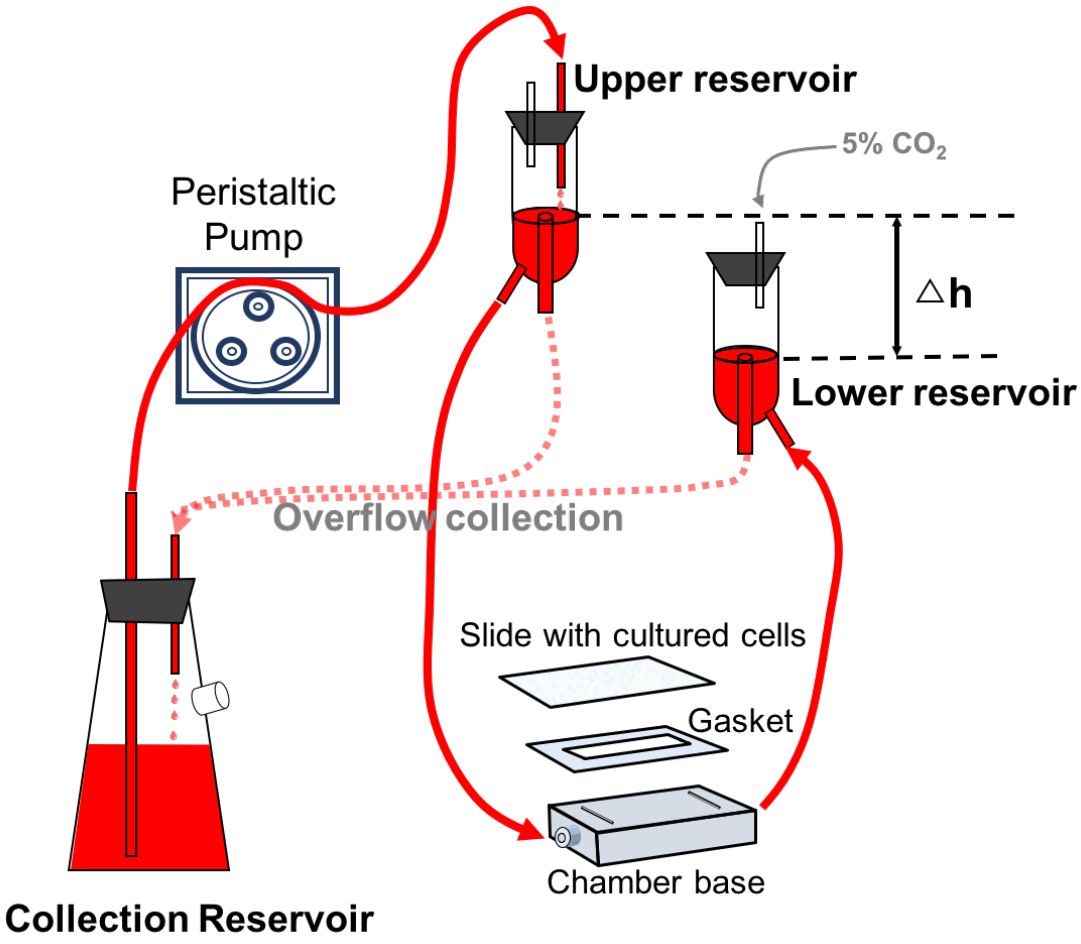

Figure 10. A schematic illustration of *in vitro* laminar flow system.

Plasmid construction and transfection

A promoter fragment of MIF (-1053~+24 bps) containing the KLF2 binding motif (CACCC) was cloned from human genomic DNA and inserted into the pGL4.20 luciferase reporter vector (Promega, Madison, WI, USA). A promoter fragment containing a mutated binding motif (CATTC) was generated using the Site-Directed Mutagenesis kit (New England Biolabs, MA, USA). AD-293 cells were co-transfected with these plasmids plus pRL-TK *Renilla* luciferase control reporter vectors at 80% confluence with Lipofectamine 2000 (Invitrogen, CA, USA) in Opti-MEM (Life Technologies, CA, USA) for 4 hours followed by 48-hour incubation in DMEM with 10% FBS. Dual-luciferase activities were detected with a dual-luciferase reporter assay and all data were normalized to *Renilla* luciferase (Promega, Madison, WI, USA).

En Face staining

All animal experiments were conducted according to protocols approved by the Institutional Animal Care and Use Committee at the University of Michigan. New Zealand white rabbits (15~20 months old) (n=4) were euthanized and immediately perfused with cold

phosphate buffered saline (PBS) containing 5 % heparin followed by cold fresh 4 % paraformaldehyde solution. Aortas were carefully dissected and fixed in 4 % PFA for another 20 minutes. After wash with cold PBS and neutralized with 100mM glycine, aortas were permeabilized with 0.2 % Triton X-100 and then incubated in blocking solution (75 mM NaCl, 18 mM Na_3 citrate, 4% FBS, 1% bovine serum albumin (BSA), 0.05% Triton X-100) for 2 hours followed by incubation with primary antibodies diluted in serum-reduced blocking solution (2 % FBS) at 4 ºC for 48 hours. Aortas were then washed in washing solution (75 mM NaCl, 18 mM Na_3 citrate, and 0.05% Triton X-100) for 1 hour and subsequently incubated with secondary antibodies for 1 hour at room temperature in dark. Aortas were washed, mounted with Prolong Gold with DAPI (Molecular Probes, OR, USA) and imaged using a Nikon A1 confocal microscope.

Chromatin immunoprecipitation assays (ChIP)

ChIP assays were performed using the EZ-ChIP Kit (EMD Millipore, MA, USA) according to the manufacturer's instruction. Briefly, HUVECs were first cross-linked with 1% formaldehyde for 10 minutes followed by glycine solution wash. Chromatin extracts were

harvested and sonicated into 500-1000 bp DNA fragments on ice. DNA fragments were then washed with protein G-agarose, centrifuged and incubated at 4 ºC with anti-KLF2 antibody (Santa Cruz Biotechnology, CA, USA) or normal anti-rabbit IgG overnight. After another incubation with protein G-agarose at 4 ºC, the immunoprecipitated complexes were washed in low-salt buffer, high-salt buffer, LiCl buffer, and Tris-EDTA buffer in order. The DNA-protein crosslinks were reversed by overnight incubation at 65 ºC with subsequent Proteinase K digestion for 1 hour at 45 ºC. Purified DNA was later collected and used as a template for real-time quantitative PCR. The primers used for the analysis of MIF promoter are:

Forward, 5'-TTGTCCTCTTCCTGCTATGTCA-3';

Reverse, 5'-GGTAAACTCGGGGACCATCTA-3'

Cell extracts and Western blotting

Confluent HUVECs were washed with cold PBS and lysed with Pierce RIPA buffer (Thermo Scientific, Rockford, IL, USA) containing protease inhibitors (Roche Applied Science, Indianapolis, IN, USA). Cell extracts were centrifuged and the supernatant was mixed with laemmli sample buffer (BIO-RAD, Hercules, CA, USA). Generally, 25

μg of protein samples were loaded per lane on a 15% SDS-PAGE gel and underwent gel electrophoresis followed by 0.2 μm nitrocellulose membrane (BIO-RAD, Hercules, CA, USA) transfer at 4 ˚C. Membranes were blocked for 1 hour at room temperature and incubated with primary antibodies at 4 ˚C overnight. After washing, membranes were incubated with a diluted (1:10, 000) IRDye-conjugated secondary antibody (Li-Cor Biotechnology, Lincoln, NE, USA) for 1 hour at room temperature. Membranes were scanned and the intensity of bands was quantified using Image Studio software (Li-Cor).

Statistical analysis

Statistical significance was assessed by unpaired Student *t* test between 2 groups and one-way ANOVA with Bonferroni post hoc test among 3 groups. A p value < 0.05 was considered statistically significant. Data are presented as mean ± SEM.

Results

Identification of shear stress sensitive genes in HCAECs

To investigate the effect of biomechanical activation on endothelial transcriptomic profile and search for novel shear stress sensitive transcripts, we first employed RNA-seq to survey the whole transcriptome of HCAECs under conditions of LS, OS and ST for 24 hours. Detected genes under different types of shear stress were compared in a pair-wise manner, including OS vs. LS, ST vs. LS, and ST vs. OS (Figure 11) at different expression cut-off (rpm>0.1 and rpm>1). A heat map of 26,973 well-expressed genes is shown in Figure 12. Next, all differentially expressed genes in each pair-wise group were sorted and underwent enrichment analysis with Kyoto Encyclopedia of Genes and Genomes (KEGG) Pathway database (Figure 13), which consists of classic metabolic as well as regulatory pathways. In this study, multiple pathways were shown to be enriched including ribosome, PI3K/Akt and Ras signaling pathways in both ST vs. LS (Figure 13A) and OS vs. LS (Figure 13B) groups; TNF and NFκB signaling pathways in OS vs. ST (Figure 13C).

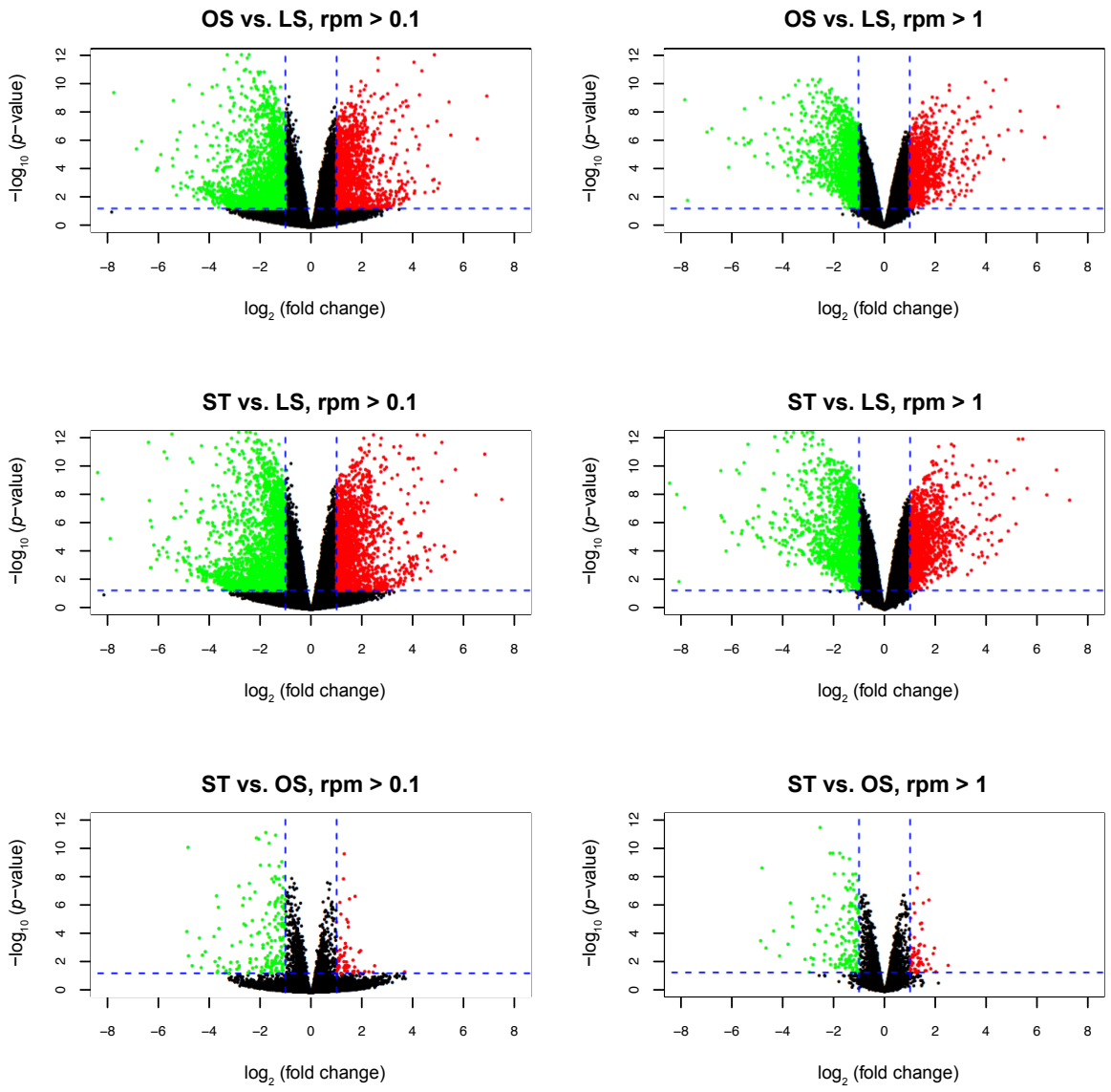

Figure 11. Identification of shear stress sensitive genes in HCAECs. Shown are volcano plots for pair-wise comparisons of genes in HCAECs under OS vs LS, ST vs LS, ST vs OS groups at different expression cut-off. y-axis is the negative $\log_{10}$ of *p* value; x-axis is the $\log_2$ of fold change. Green dots represent genes with significant *p* value and negative $\log_2$ of fold change; red dots represent genes with significant *p* value and positive $\log_2$ of fold change; black dots represent genes with no significant *p* value. A Banjamini-Hochberg corrected $p < 0.05$ was considered as statistically significant.

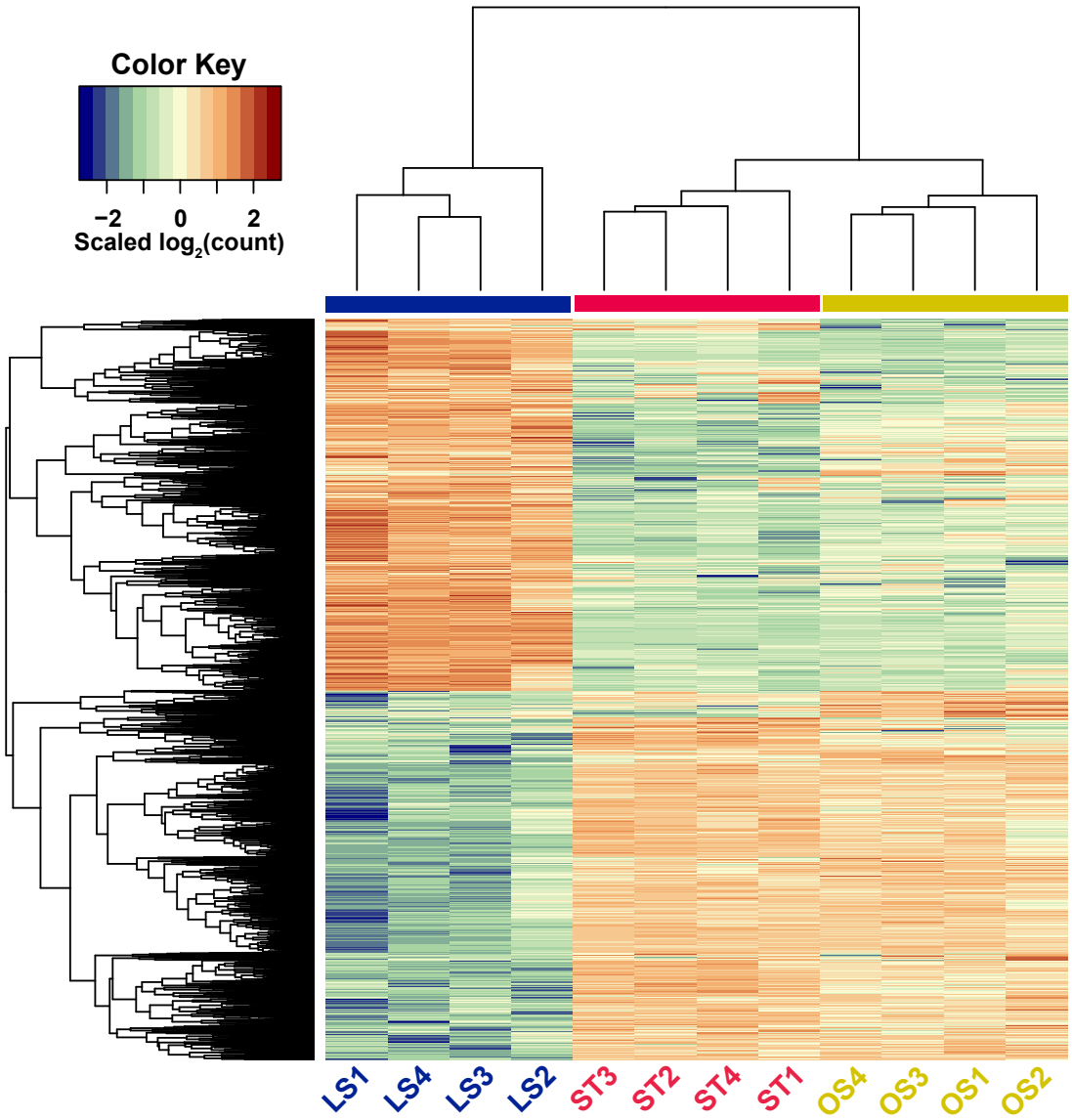

Figure 12. Heat map of all detected genes in HCAECs under ST, OS and LS conditions.

A

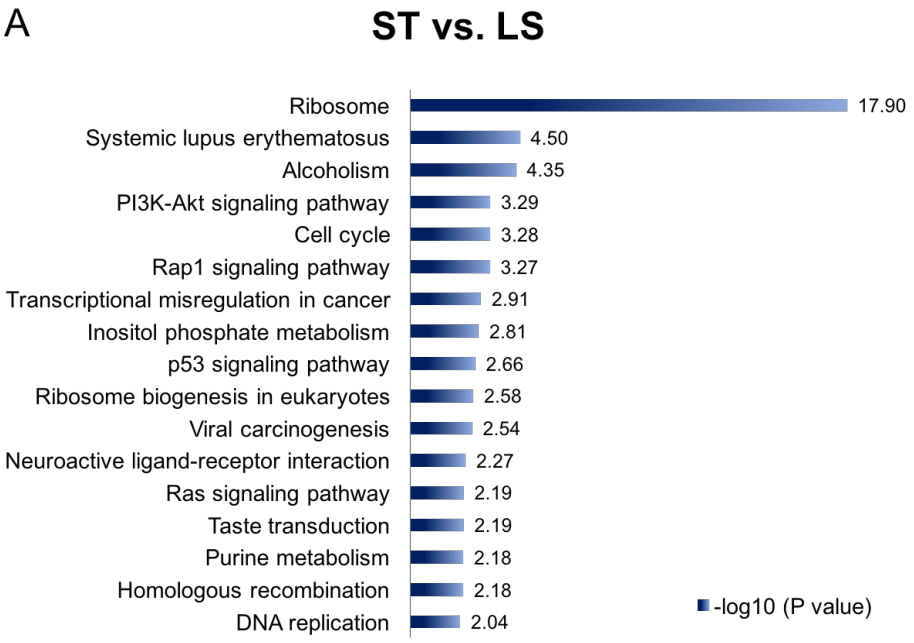
ST vs. LS
Ribosome 17.90
Systemic lupus erythematosus 4.50
Alcoholism 4.35
PI3K-Akt signaling pathway 3.29
Cell cycle 3.28
Rap1 signaling pathway 3.27
Transcriptional misregulation in cancer 2.91
Inositol phosphate metabolism 2.81
p53 signaling pathway 2.66
Ribosome biogenesis in eukaryotes 2.58
Viral carcinogenesis 2.54
Neuroactive ligand-receptor interaction 2.27
Ras signaling pathway 2.19
Taste transduction 2.19
Purine metabolism 2.18
Homologous recombination 2.18
DNA replication 2.04
-log10 (P value)

B

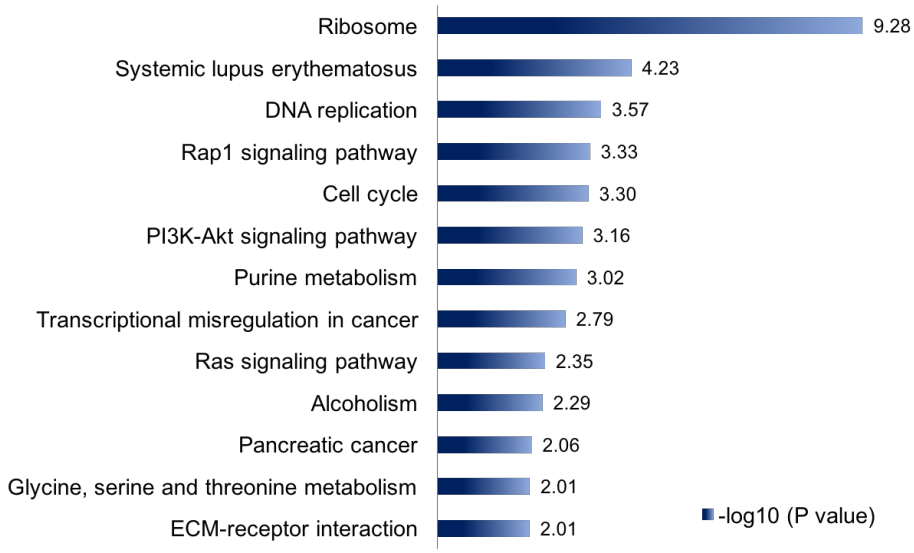
OS vs. LS
Ribosome 9.28
Systemic lupus erythematosus 4.23
DNA replication 3.57
Rap1 signaling pathway 3.33
Cell cycle 3.30
PI3K-Akt signaling pathway 3.16
Purine metabolism 3.02
Transcriptional misregulation in cancer 2.79
Ras signaling pathway 2.35
Alcoholism 2.29
Pancreatic cancer 2.06
Glycine, serine and threonine metabolism 2.01
ECM-receptor interaction 2.01
-log10 (P value)

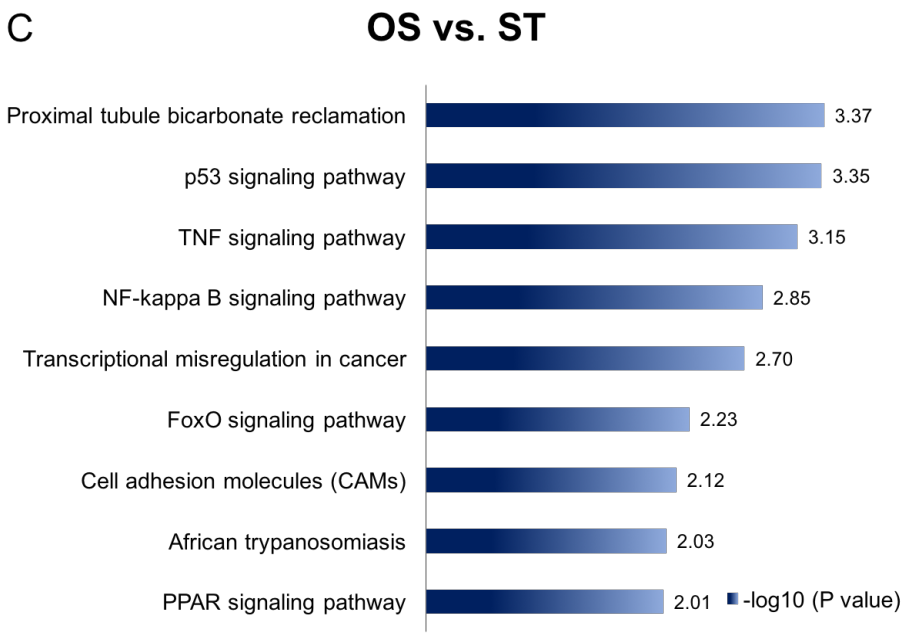

Figure 13. Kyoto Encyclopedia of Genes and Genomes (KEGG) enrichment analysis. Shown are enriched signaling pathways in ST vs. LS **(A)**, OS vs. LS **(B)**, ST vs. OS **(C)** annotated in KEGG Pathway database with a value of $P < 0.01$.

Transcriptomic profiling reveals a wide range of differentially expressed inflammation-related genes in response to shear stress

There were over 6,000 differentially expressed genes in response to different types of shear stress. It is unlikely to investigate them all in this present work. We thus focus on the shear stress-induced pro-/anti-inflammatory genes in ECs considering that atherosclerosis is well-recognized as a chronic inflammatory disease[151]. Factors that are documented in the inflammation category by Gene Ontology

function annotation were demonstrated as a volcano plot (Figure 14A). Notably, pro-inflammatory factors such as FABP4, CXCR4 were significantly upregulated whereas anti-inflammatory factors including cyclooxygenase 2 (COX2) and KLF4 were markedly down-regulated in ECs under ST condition comparing to those under LS condition (Figure 14A). A heat map of all differentially expressed genes in inflammation category is shown in Figure 14B, which revealed that gene expression pattern in ECs under LS condition were completely different from those under OS and ST conditions.

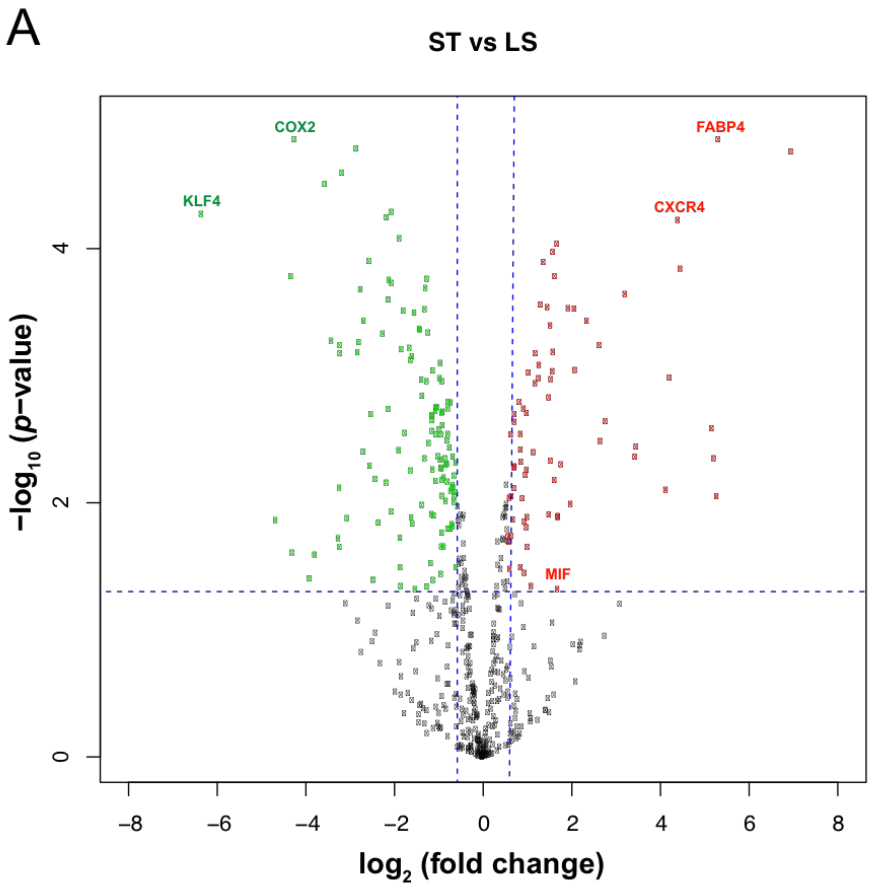

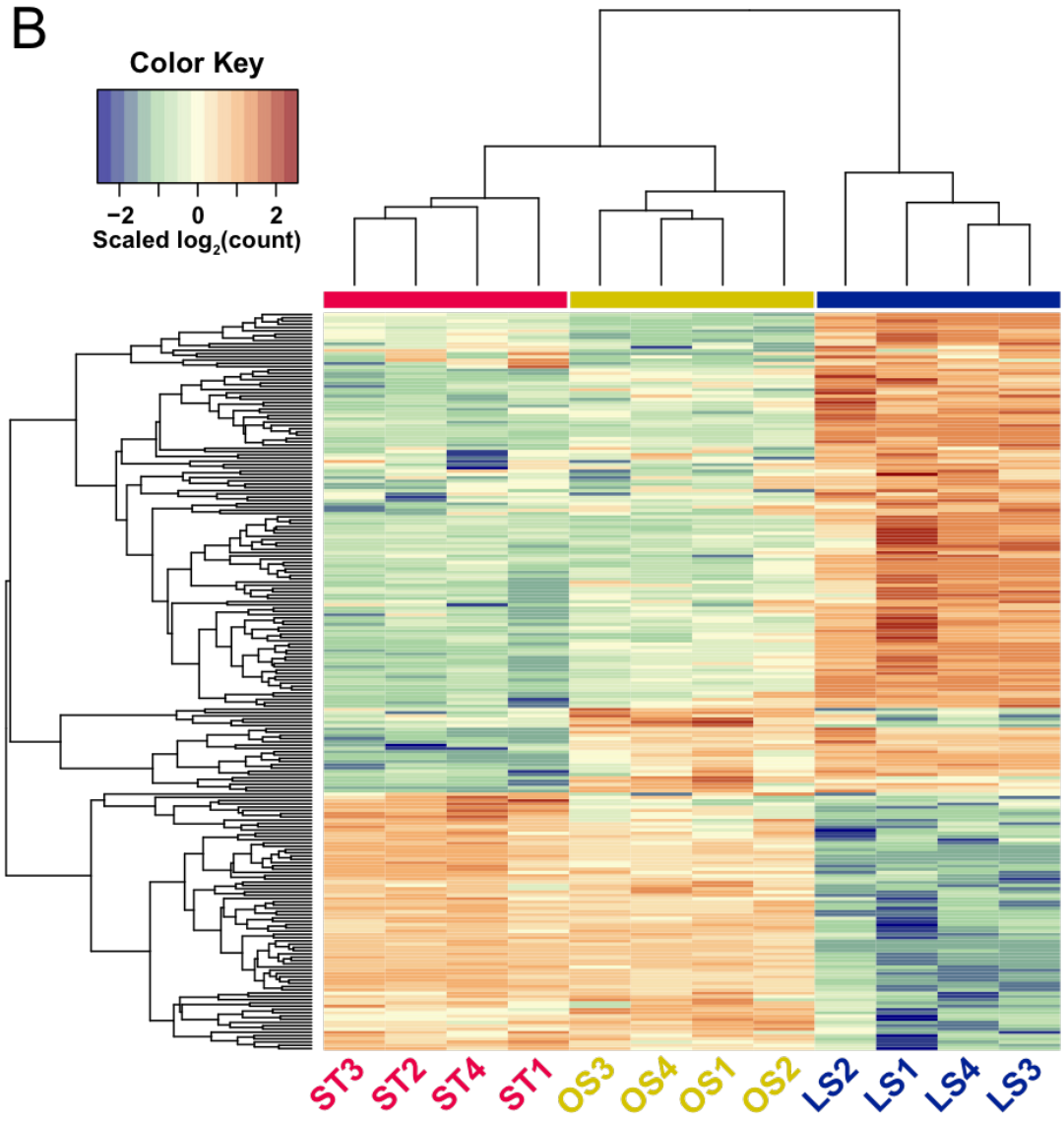

Figure 14. Modulation of genes in inflammation category in response to different types of shear stress. **(A)** Volcano plot of all the inflammation-related genes detected in HCAECs. y-axis is the negative $\log_{10}$ of *p* value; x-axis is the $\log_2$ of fold change. Green dots represent genes downregulated in ECs under ST condition with significant *p* value; red dots represent genes upregulated in ECs under ST condition with significant *p* value; black dots represent genes with no significant *p* value. **(B)** Heat map of all the inflammation-related genes that are differentially expressed in HCAECs under ST conditions.

Pro-inflammatory cytokine MIF is sensitive to shear stress and co-localizes with OS in the arterial tree

Interestingly, I found a novel pro-inflammatory factor MIF that is sensitive to shear stress based on our RNA-seq data (Figure 14A). MIF has been implicated in multiple inflammatory diseases including atherosclerosis[199]. The transcript level of MIF was confirmed by qPCR result (Figure 15A), which showed a nearly 2-fold difference in MIF expression in HCAECs under LS condition compared to ST or OS conditions. To assess MIF expression in other ECs, human umbilical vein ECs (HUVECs) were used to demonstrate a reduced protein level of MIF under LS (Figure 15B and 15C). Next, I asked if MIF is associated with flow pattern *in vivo*, which varies spatially in the arterial tree. Aorta from New Zealand white rabbits fed on a chow diet were harvested for *en face* immunostaining. Consistent with the *in vitro* data, a high level of MIF immunoreactivity was detected in OS-exposed regions including lesser curvature as well as bifurcation areas while the level of MIF was barely detected in straight descending aorta where LS exists (Figure 15D). Taken together, RNA-seq data revealed that MIF is a novel shear stress-sensitive cytokine, the expression of which is high in atherosclerotic-prone

areas and is low in athero-resistant segments *in vivo*, suggesting a potential role of MIF in OS-induced endothelial dysfunction.

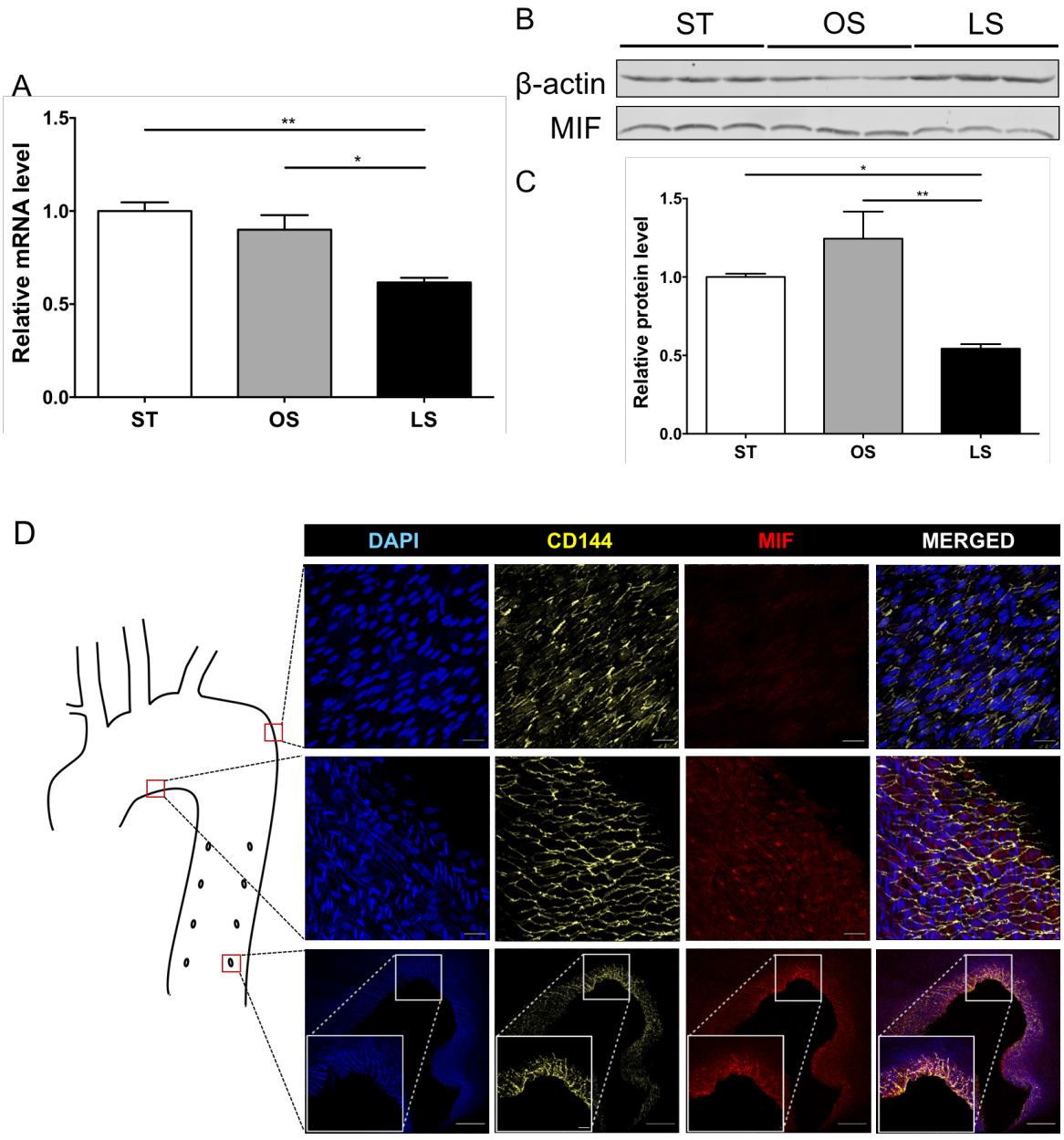

Figure 15. MIF expression in ECs can be regulated by shear stress. The transcript level of MIF detected by qPCR **(A)** in human coronary artery endothelial cells (HCAECs) after 24-hour exposure to static (ST) culture, oscillatory shear stress (OS) and laminar shear stress (LS) (n=4). Representative immunoblot **(B)** and the band intensity quantification **(C)** of

MIF protein level in human umbilical endothelial cells (HUVECs) after 24-hour exposure to ST, OS and LS (n=3). In all bar graphs, data are shown as mean ± SEM. *P<0.05, **P<0.01. **(D)** A cartoon showing the different parts of rabbit aorta (n=4) that underwent *en face* immunostaining with anti-CD144 (yellow) and anti-MIF (red) and DAPI (blue). Scale bar = 100 μm.

MIF is transcriptionally regulated by KLF2

Given the high expression of the pro-inflammatory MIF in OS predominant areas, we asked if it can be regulated by shear stress-sensitive transcription factors in ECs, including the first reported shear stress-induced transcription factor KLF2[161], which functions as a master regulator of EC proliferation, thrombosis and inflammation. Thus, we first searched for shear stress-sensitive KLF family members that are also involved in inflammation. In addition to KLF2, KLF4 and KLF11 have been implicated in inflammation in ECs as well[209-211]. Thus, we detected the transcript level of MIF in cultured HUVECs overexpressed with KLF2, KLF4 and KLF11 respectively. MIF mRNA levels were down-regulated only by KLF2 overexpression, no significant difference was observed in KLF4- and KLF11-overexpressed ECs (Figure 16A). We used human MIF ELISA assay to exam the secreted MIF in culture medium after 48 hours incubation with serum-free medium (Figure 16B). The level of secreted MIF was

significantly higher in KLF2 overexpressed group than the control group. The protein level of MIF was significantly reduced in ECs infected with adenovirus-KLF2 compared to the one with adenovirus-GFP infection (Figure 16C and 16D).

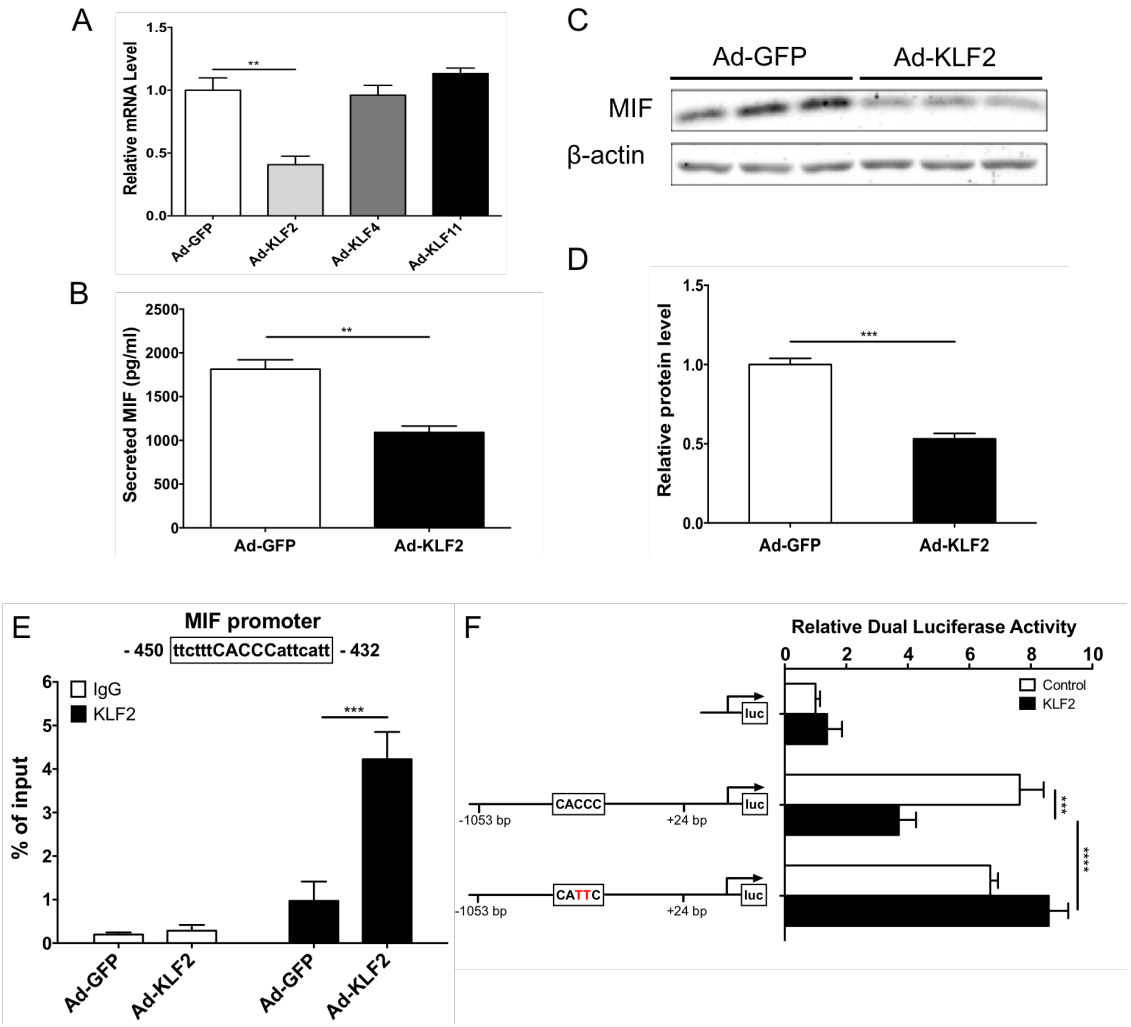

Figure 16. MIF is transcriptionally regulated by KLF2. **(A)** MIF mRNA level in HUVECs determined by qPCR after 48-hour adenovirus-mediated overexpression of KLF2, KLF4 and KLF11 (n=3). mRNA expression was normalized to HPRT mRNA. **(B)** The secreted MIF level of HUVECs after 48-hour incubation with serum-free medium (n=6). A total of $2x10^5$ cells were counted and seeded into each well for the following secreted MIF ELISA. **(C)** Representative Western blot showing the expression of MIF, the loading

control β-actin in ECs overexpressing KLF2 or GFP (n=3). **(D)** the quantitative analysis of band intensity from western blot. **(E)** HUVECs were infected with adenovirus-KLF2 or -GFP for 72 hours. ChIP assay was performed using a rabbit antibody against KLF2 and equivalent amount of rabbit IgG as control. The binding of KLF2 to the MIF promoter was determined by qPCR. **(F)** Dual luciferase activity were assessed in Ad293 using the 1-kB MIF-Luc promoter construct and the mutated one in combination with expression plasmids for KLF2. Mutation of the indicated binding sites was performed using the Site-Directed Mutagenesis kit. Data represent relative luciferase activity (normalized to *Renilla* luciferase), n=6 per group. Data are shown as mean ± SEM. **P<0.01, ***P<0.001, ****P<0.0001.

To determine the regulatory mechanism of KLF2 to inhibit MIF expression, I performed chromatin immunoprecipitation by using anti-KLF2 antibody and assessed its effect on MIF promoter activity. We found that KLF2 directly binds to a specific site in the MIF promoter region (Figure 16E). and inhibits the promoter activity of MIF (Figure 16F). Mutation of KLF2 binding site abolished the reduction of relative luciferase activity (Figure 16F).

KLF2 knockdown in ECs attenuates LS-induced inhibition of MIF

To test the effect of KLF2 in LS-induced inhibition of MIF, HUVECs were infected with adenovirus-shKLF2 to knockdown the endogenous KLF2 levels and were exposed to LS for 24 hours. KLF2 mRNA level was reduced to almost 50% in HUVECs under LS

condition (Figure 17A) and MIF was significantly increased in KLF2 knockdown group at both transcript level (Figure 17B) and protein level (Figure 17C).

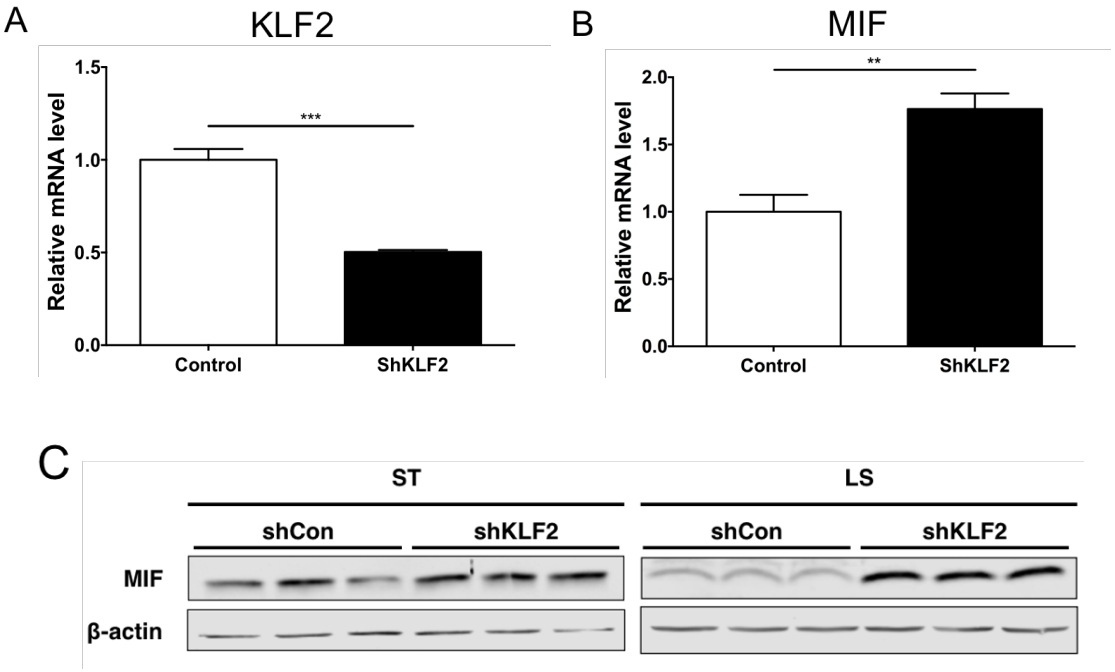

Figure 17. Knockdown of KLF2 attenuates LS-induced reduction of MIF. HUVECs were transfected with adenovirus-shKLF2 or -control for 48 hours before LS stimulation for 24 hours. The transcript level of KLF2 **(A)** and MIF **(B)** were detected by qPCR. Representative Western blot of MIF and β-actin in ECs infected with adenovirus-shKLF2 or -control under static culture or LS conditions. Data shown are presented as mean ± SEM. **P<0.01, ***P<0.001.

Discussion

Cardiovascular disease is the top killer in the United States and worldwide, contributing to roughly 1/3 of mortality globally[212]. Atherosclerosis characterized by the deposition of circulating lipid, the infiltration of

leukocytes and the aberrant proliferation and apoptosis rate of ECs and SMCs is recognized as the fundamental basis of ischemic heart disease and stroke[128]. There are numerous studies investigating the pathogenesis of atherosclerosis, one focus of which is on the hemodynamic force generated by blood flow. Here, we analyzed RNA-seq data and discovered a novel shear stress sensitive cytokine MIF. MIF can be upregulated by OS, but downregulated by LS indicating its potential role in the process of atherosclerosis in that the atherosclerotic lesions preferentially develop in OS predominant areas. In fact, multiple lines of evidence have demonstrated that MIF may be an atherogenic cytokine that correlates with increased vessel wall thickening and lipid deposition in the aorta of western diet-fed rabbit, atherosclerotic-prone mouse model, and human patients with severe atherosclerotic lesions[200,201,213]. The present work has added another piece of evidence to help elucidate the molecular basis of MIF's role in the development of atherosclerosis. MIF itself can act as a ligand and binds to its receptors, CXCR2 and CXCR4, on the endothelial surface membrane to activate downstream inflammatory signaling pathways, leading to the recruitment of T cells and macrophages[204]. By blocking endothelial MIF with monoclonal antibody, Schober et al. have reported a stabilized plaque phenotype with reduced foam cells and increased VSMC[214]. Overall, MIF

plays a critical role in the initiation and progression of atherosclerosis. The shear stress-sensitive characteristic of MIF may help to understand the pathology of atherosclerosis from a biomechanical perspective.

KLF2 is a key transcription factor that involves in multiple biological processes, including inflammation and thrombosis. Most importantly, it is a master regulator induced by shear stress[215]. In addition to the regulation of eNOS, KLF2 is well-evidenced to modulate thrombomodulin, plasminogen activator inhibitor, and cytokine-stimulated tissue factor[160]. In this study, KLF2 has been shown to regulate endothelial MIF by directly binding to its specific binding site 5'-CACCC-3' in the MIF promoter. Knockdown of KLF2 can potently attenuate the LS-mediated inhibition of MIF, suggesting a naturally protective role of KLF2 in the endothelium. In fact, endogenous molecules in cells or in circulating blood may become promising therapeutic targets for drug development. One good example is the protective effects induced by exercise. Physical exercise is widely recognized to reduce the risk of cardiovascular diseases. Besides depletion of the intracelullar energy pool, exercise also increases the velocity of blood flow, which subsequently elevates the magnitude of shear stress, exerting atheroprotective forces[152].

Here, the whole endothelial transcriptome was profiled under ST, OS and LS conditions by RNA-seq. This profiling revealed a large amount of novel shear sensitive genes and lncRNAs that have not been previously reported. This work provides an easy access to the whole transcriptome pool and informs future searches for novel targets for anti-atherosclerosis drug development. However, it is important to note that there are several limitations to this study. One concern is the temporal factor. Exposure time to shear stress is essential in signaling pathway activation and subsequent gene expression. We exposed HCEACs to different types of shear stress for 24 hours, however, others have reported that transient or short-term exposure to shear stress induces a distinct set of gene expression[161,216]. It would be of great interest to profile the endothelial transcriptome at different time points to yield a comprehensive understanding of the dynamic change in ECs in response to shear stress. Another limitation of this study is that the RNA-seq kit used generates a 50-nucleotide (nt) paired end and assemble a 200 nt read, which doesn't include the shear stress-induced changes of microRNAs, the size of which is approximately 23 nt[217]. The function and regulation of known mechanosensitive microRNAs have been reviewed[218,219], however, it will be very useful to obtain the microRNA profile in ECs under shear stress.

CHAPTER IV

Discussion and future directions

With generous and unlimited help from my colleagues and others, I investigated the endothelial transcriptomic profile under different types of shear stress, including ST, OS and LS. I compared the differentially expressed genes under ST vs. LS, OS vs. LS and ST vs. OS and found a large variety of genes that are influenced by shear stress. There are over 6,000 genes that are differentially expressed in either ST vs. LS or OS vs. LS. Interestingly, transcriptomic profile reveals that ECs under ST condition are very similar to those under OS condition and both are different from ECs under LS condition. Considering that ECs are constantly exposed to blood flow *in vivo*, the LS condition is regarded as normal for ECs. Thus, the endothelial transcriptome under both the OS and ST conditions deviates from the one under the LS condition, suggesting that both OS and ST are pathologically relevant. Next, I sought to confirm this similarity by showing the biological evidence. I picked some well-known shear stress sensitive genes, including eNOS, ID1 and KLF2 to verify our results with previous

reports[161,216,220]. I also included some novel shear sensitive genes that are implicated in critical biological processes such as KLF11 in inflammation[210], TEK, ANGPT2 in angiogenesis[221] to confirm the validity of our RNA-seq results. Then I compared the transcript levels of these selected genes by qPCR and their protein levels by Western blot, which in turn supported the similarity of ECs under ST and OS conditions.

Following RNA-seq analysis, differential expression analysis was performed to sort out the shear stress-induced differentially expressed genes with important biological significance. KEGG signaling pathways enrichment analysis has highlighted the signaling pathways that are activated under different shear stress conditions. I decided to focus on the inflammation category due to the natural inflammatory process of atherosclerosis. Several well-known shear stress sensitive genes with strong pro-/anti-inflammatory properties have been revealed, including KLF4, COX2, FABP4 and CXCR4. Among them, MIF was the one with known pro-inflammatory as well as pro-atherosclerotic effects, but new in the category of shear stress sensitive genes. Hence, I decided to investigate regulatory mechanisms in ECs to provide an understanding of MIF expression in response to biomechanical activation. I found that KLF2 regulates MIF expression in ECs.

Overexpression of KLF2 substantially inhibits MIF transcription, translation, and secretion. To further determine the molecular basis of KLF2-mediated regulation of MIF, I performed ChIP and dual luciferase assays targeting the specific KLF2 binding sites in the MIF promoter and illustrated that MIF inhibition is directly regulated by KLF2-binding. This novel finding owes to the large transcriptomic profile provided by RNA-seq. It would have been difficult to link transcription factor KLF2 to MIF modulation otherwise.

Endothelial biology in cell culture

Cell culture is considered to be a powerful and easy-to-handle tool for cell biology studies. Modified cell growth medium and precise control of temperature, pH, and osmolarity enables cell culture to better emulate the physiological condition. Numerous studies have informed endothelial biology based on the research on ECs in static culture. However, primary cultured ECs have been observed to dramatically lose endothelial characteristics and consistency in response to stimuli after certain passages despite the same growth medium and environment. In addition, there is an increasing awareness that basic research cannot be translated into drug development and clinical application, giving rise to the question if cell

biology is the correct research approach. One good example is the development of statin drugs. The first experimental drug compactin did not work in rats but was highly effective in dogs and monkeys, indicating the priority of the right experimental animal model for specific disease[222]. In endothelial biology, the lack of biomechanical activation may be a reason for the untranslatable discoveries from cultured ECs. Based on observations from clinical perspectives, I speculate that ST conditions may mimic the severe ischemic conditions in the coronary or carotid arteries, where ECs in the distal areas to the obstruction suffer from a lack of shear stress stimulation. Hence, I hypothesize that the ST condition itself may provide a pathological environment for ECs and provoke pro-inflammatory forces, leading to endothelial dysfunction.

In vitro flow simulation system

It is reasonable to argue that biomechanical stimulation should be included in cultured ECs for accurate endothelial biology studies. A large variety of in vitro flow systems for cultured ECs have been developed to simulate in vivo flow environments. Laminar shear stress can be simulated by using a gravity-based flow system as

shown in Figure 10. It requires one upper reservoir and one lower reservoir to provide height difference for the generation of the optimal flow rate. A peristaltic pump is required to pump medium from the collection reservoir into the upper reservoir. Both upper and lower reservoirs require over flow exits to avoid the volume limit and reuse the medium. Each reservoir is equipped with an open glass tube in the rubber plug to maintain the atmospheric pressure and the carbon dioxide supplementation. In the cell chamber, cells at confluency on the culture plate are inversely placed towards the chamber side with a 0.2 mm silicone gasket in the middle. I use stainless steel clamp to seal the chamber after the clearance of air bubbles. In our system, a 13 cm height difference can produce a roughly 85 ml/min flow rate, or a 15 dyne/cm^2 shear stress force. ECs in the chamber become elongated and oriented with the direction of flow can be observed as soon as 12 hours later, consistent with previous studies[111].

Hanjoong Jo's group and others[223] use a rotating Teflon cone (0.5° cone angle) on a 100 mm dish to generate LS controlled by a stepping motor and a computer program. This system can also produce OS by rotating the cone clockwise and counterclockwise in

a repeated cycle with the same motor-computer system. Additional flow systems, including an orbital shaker-based shear stress simulation system, are also used for cell research purposes[123,224,225]. However, due to the various flow velocities from the center to the edge of the plate, this system fails to produce a uniform shear stress across the entire endothelial monolayer. The difference in magnitude of shear stress, especially those overlapping the low and high shear stress threshold, may contribute to the heterogeneity in endothelial function.

Potential therapeutic drug targets

Therapeutic development for cardiovascular disease is at a crossroads where low productivity meets more funding demand every year. Since the availability of statin drugs in 1987[222], the death rate from cardiovascular disease, especially from ischemic heart disease, has markedly decreased whereas the economic burden and risk factors remain high[212]. Understanding the molecular mechanisms of atherosclerosis, which is the major fundamental basis of ischemic heart disease and stroke, is the key to lowering the risk of cardiovascular disease. Here, I performed RNA-seq to profile the

transcriptome of ECs under shear stress. This transcriptomic analysis provides a large amount of gene expression information including the adaptive response of protein-coding genes as well as non-coding RNAs under different types of shear stress. Investigation of shear stress-sensitive genes as well as the interaction between signaling molecules may help the community to find new potential therapeutic target to treat atherosclerosis. My colleagues and I are dedicated to surveying the shear stress-induced modulation of protein-coding genes and lncRNAs. Haocheng in our lab works on the transcription factor EB (TFEB), which is well documented as a key role in the regulation of autophagy[226]. RNA-seq data revealed that TFEB can be regulated by shear stress in ECs. Genes that are only up-regulated by OS might be of particular interest in that OS has been shown to induce the initiation of atherosclerosis in the vascular intima[166].

Shear stress sensitive lncRNA and its role in atherosclerosis

LncRNAs are groups of non-coding RNAs longer then 200 nucleotides. The emergence of lncRNA has opened a new chapter of RNA-DNA, RNA-RNA, RNA-protein interaction in transcriptional regulation[177]. The elucidation of the capability of each lncRNA has a

long way to go, but the evidence that lncRNA is actively involved in chromatin modification, transcriptional regulation and post-transcriptional regulation[172] draws everyone's attention. In our RNA-seq data, there is a long list of lncRNAs that are influence by shear stress. Despite the novelty of lncRNA, the lack of proper research tools and reagents becomes a hurdle for studying lncRNA. My colleague and I picked several lncRNA candidates and performed a few preliminary experiments but the outcome is not as good as we expected. The antisense oligonucleotides we obtained commercially to knockdown lncRNA in ECs were not efficient and sometimes exerted toxicity on ECs with a higher concentration. However, the potential application of lncRNA as a therapeutic target for cardiovascular disease is of huge interest and with new tools and revolutionary technology, the lncRNA biology may be elucidated in the near future. Several pioneer groups have published some exciting reports regrarding lncRNA in cardiovascular disease. Kumarswamy et al. have reported that a human circulating lncRNA LIPCAR was down-regulated at early stage of myocardial infarction and up-regulated over time[227]. Han et al. discovered a cluster of lncRNA from Myh7 loci named as myosin heavy-chain-associated RNA transcripts

(Mhrt). They show that Mhrt is cardiac specific and may involve in the protection from cardiomyopathy[228]. In regards to EC biology, the lncRNA MALAT1 has been implicated in vascular growth[189] and in high glucose-induced inflammatory process[179].

Summary

This present work provides a board view of biomechanical activation in ECs and its effect on endothelial biology. Transcriptomic profiling of ECs sheds light on the transcriptome differences among ECs under ST, OS and LS conditions. My work highlights the power of RNA-seq in discovering novel shear stress-sensitive genes in ECs under athero-protective LS as well as athero-prone OS conditions, which may provide the community with novel potential therapeutic targets for treating atherosclerosis from a biomechanical perspective. Future studies should focus on other novel shear stress-modulated genes in endothelial biology and explore the function of shear stress-sensitive lncRNA in ECs. Elucidating the molecular mechanisms of shear stress-mediated modulation of endothelial function may provide insights into the pathogenesis of atherosclerosis as well as advance the cardiovascular medicine.

Bibliography

1. Ku, D. N. Blood flow in arteries. *Annual Review of Fluid Mechanics* **29,** 399–434 (1997).
2. Fung, Y. *Biomechanics: circulation*. (2013).
3. Cassanova, R. A. & Giddens, D. P. Disorder distal to modeled stenoses in steady and pulsatile flow. *Journal of Biomechanics* **11,** 441–453 (1978).
4. Budwig, R., Elger, D., Hooper, H. & Slippy, J. Steady Flow in Abdominal Aortic Aneurysm Models. *J Biomech Eng* **115,** 418–423 (1993).
5. Chiu, J.-J. & Chien, S. Effects of disturbed flow on vascular endothelium: pathophysiological basis and clinical perspectives. *Physiological Reviews* **91,** 327–387 (2011).
6. Chatzizisis, Y. S. *et al.* Role of endothelial shear stress in the natural history of coronary atherosclerosis and vascular remodeling: molecular, cellular, and vascular behavior. *Journal of the American College of Cardiology* **49,** 2379–2393 (2007).
7. Cheng, C. *et al.* Large variations in absolute wall shear stress levels within one species and between species. *Atherosclerosis* **195,** 225–235 (2007).
8. Sutera, S. P. & Skalak, R. The history of Poiseuille's law. *Annual Review of Fluid Mechanics* (1993).
9. Stroev, P. V., Hoskins, P. R. & Easson, W. J. Distribution of wall shear rate throughout the arterial tree: a case study. *Atherosclerosis* **191,** 276–280 (2007).
10. Traub, O. & Berk, B. C. Laminar shear stress mechanisms by which endothelial cells transduce an atheroprotective force. *Arteriosclerosis* (1998). doi:10.1161/01.ATV.18.5.677
11. Li, Y.-S. J., Haga, J. H. & Chien, S. Molecular basis of the effects of shear stress on vascular endothelial cells. *Journal of Biomechanics* **38,** 1949–1971 (2005).
12. Wang, N., Butler, J. P. & Ingber, D. E. Mechanotransduction across the cell surface and through the cytoskeleton. *Science* **260,** 1124–1127 (1993).
13. Tzima, E. *et al.* A mechanosensory complex that mediates the endothelial cell response to fluid shear stress. *Nature* **437,** 426–431 (2005).

14. Shyy, J. & Chien, S. Role of integrins in endothelial mechanosensing of shear stress. *Circulation Research* (2002). doi:10.1161/01.RES.0000038487.19924.18
15. Hierck, B. P. *et al.* Primary cilia sensitize endothelial cells for fluid shear stress. *Developmental Dynamics* **237,** 725–735 (2008).
16. Conway, D. E. *et al.* Fluid shear stress on endothelial cells modulates mechanical tension across VE-cadherin and PECAM-1. *Curr. Biol.* **23,** 1024–1030 (2013).
17. Berthiaume, F. & Frangos, J. A. Fluid flow increases membrane permeability to merocyanine 540 in human endothelial cells. *Biochimica et Biophysica Acta (BBA)- …* **1191,** 209–218 (1994).
18. Gudi, S., Nolan, J. P. & Frangos, J. A. Modulation of GTPase activity of G proteins by fluid shear stress and phospholipid composition. *Proc. Natl. Acad. Sci. U.S.A.* **95,** 2515–2519 (1998).
19. Butler, P. J., Tsou, T.-C., Li, J. Y.-S., Usami, S. & Chien, S. Rate sensitivity of shear-induced changes in the lateral diffusion of endothelial cell membrane lipids: a role for membrane perturbation in shear-induced MAPK activation. *FASEB J.* **16,** 216–218 (2002).
20. van Haaren, P. M. A., VanBavel, E., Vink, H. & Spaan, J. A. E. Localization of the permeability barrier to solutes in isolated arteries by confocal microscopy. *Am. J. Physiol. Heart Circ. Physiol.* **285,** H2848–H2856 (2003).
21. Megens, R. T. A. *et al.* Two-photon microscopy of vital murine elastic and muscular arteries. Combined structural and functional imaging with subcellular resolution. *J. Vasc. Res.* **44,** 87–98 (2007).
22. Reitsma, S., Slaaf, D. W., Vink, H., van Zandvoort, M. A. M. J. & oude Egbrink, M. G. A. The endothelial glycocalyx: composition, functions, and visualization. *Pflugers Arch.* **454,** 345–359 (2007).
23. Mochizuki, S. *et al.* Role of hyaluronic acid glycosaminoglycans in shear-induced endothelium-derived nitric oxide release. *Am. J. Physiol. Heart Circ. Physiol.* **285,** H722–6 (2003).
24. Satir, P., Pedersen, L. B. & Christensen, S. T. The primary cilium at a glance. *J. Cell. Sci.* **123,** 499–503 (2010).
25. Van der Heiden, K. *et al.* Endothelial primary cilia in areas of disturbed flow are at the base of atherosclerosis. *Atherosclerosis* **196,** 542–550 (2008).
26. Iomini, C., Tejada, K., Mo, W., Vaananen, H. & Piperno, G. Primary cilia of human endothelial cells disassemble under laminar shear stress. *J. Cell Biol.* **164,** 811–817 (2004).
27. Nauli, S. M. *et al.* Endothelial cilia are fluid shear sensors that

regulate calcium signaling and nitric oxide production through polycystin-1. *Circulation* **117,** 1161–1171 (2008).
28. Hynes, R. O. Integrins: versatility, modulation, and signaling in cell adhesion. *Cell* **69,** 11–25 (1992).
29. Jalali, S. *et al.* Integrin-mediated mechanotransduction requires its dynamic interaction with specific extracellular matrix (ECM) ligands. *Proc. Natl. Acad. Sci. U.S.A.* **98,** 1042–1046 (2001).
30. Wang, Y. *et al.* Interplay between integrins and FLK-1 in shear stress-induced signaling. *AJP: Cell Physiology* **283,** C1540–7 (2002).
31. Schlaepfer, D. D. & Hunter, T. Integrin signalling and tyrosine phosphorylation: just the FAKs? *Trends Cell Biol.* **8,** 151–157 (1998).
32. Parsons, J. T. & Parsons, S. J. *Src family protein tyrosine kinases: cooperating with growth factor and adhesion signaling pathways*. (Current opinion in cell biology, 1997).
33. Li, S. *et al.* Fluid shear stress activation of focal adhesion kinase. Linking to mitogen-activated protein kinases. *Journal of Biological Chemistry* **272,** 30455–30462 (1997).
34. Jalali, S. *et al.* Shear stress activates p60src-Ras-MAPK signaling pathways in vascular endothelial cells. *Arterioscler Thromb Vasc Biol* **18,** 227–234 (1998).
35. Fleming, I., Fisslthaler, B., Dixit, M. & Busse, R. Role of PECAM-1 in the shear-stress-induced activation of Akt and the endothelial nitric oxide synthase (eNOS) in endothelial cells. *J. Cell. Sci.* **118,** 4103–4111 (2005).
36. Osawa, M., Masuda, M., Kusano, K.-I. & Fujiwara, K. Evidence for a role of platelet endothelial cell adhesion molecule-1 in endothelial cell mechanosignal transduction: is it a mechanoresponsive molecule? *J. Cell Biol.* **158,** 773–785 (2002).
37. Nilius, B. & Droogmans, G. Ion channels and their functional role in vascular endothelium. *Physiological Reviews* **81,** 1415–1459 (2001).
38. Olesen, S. P., Claphamt, D. & Davies, P. Haemodynamic shear stress activates a K+ current in vascular endothelial cells. *Nature* (1988).
39. Hoger, J. H., Ilyin, V. I., Forsyth, S. & Hoger, A. Shear stress regulates the endothelial Kir2.1 ion channel. *Proc. Natl. Acad. Sci. U.S.A.* **99,** 7780–7785 (2002).
40. Adams, D. J., Barakeh, J., Laskey, R. & Van Breemen, C. Ion channels and regulation of intracellular calcium in vascular endothelial cells. *The FASEB Journal* **3,** 2389–2400 (1989).
41. Jo, H. *et al.* Differential effect of shear stress on extracellular signal-

regulated kinase and N-terminal Jun kinase in endothelial cells. Gi2- and Gbeta/gamma-dependent signaling pathways. *Journal of Biological Chemistry* **272,** 1395–1401 (1997).
42. Chachisvilis, M., Zhang, Y.-L. & Frangos, J. A. G protein-coupled receptors sense fluid shear stress in endothelial cells. *Proc. Natl. Acad. Sci. U.S.A.* **103,** 15463–15468 (2006).
43. Schlessinger, J. Receptor tyrosine kinases: legacy of the first two decades. *Cold Spring Harb Perspect Biol* **6,** (2014).
44. Chen, K. D. *et al.* Mechanotransduction in response to shear stress. Roles of receptor tyrosine kinases, integrins, and Shc. *Journal of Biological Chemistry* **274,** 18393–18400 (1999).
45. Jin, Z.-G. *et al.* Ligand-independent activation of vascular endothelial growth factor receptor 2 by fluid shear stress regulates activation of endothelial nitric oxide synthase. *Circulation Research* **93,** 354–363 (2003).
46. Pearson, J. D. Endothelial cell biology. *Radiology* (1991). doi:10.1523/JNEUROSCI.2755-05.2006
47. Kim, E. K. & Choi, E.-J. Pathological roles of MAPK signaling pathways in human diseases. *Biochim. Biophys. Acta* **1802,** 396–405 (2010).
48. Liu, Y., Yin, G., Surapisitchat, J., Berk, B. C. & Min, W. Laminar flow inhibits TNF-induced ASK1 activation by preventing dissociation of ASK1 from its inhibitor 14-3-3. *J. Clin. Invest.* **107,** 917–923 (2001).
49. Zakkar, M. *et al.* Increased endothelial mitogen-activated protein kinase phosphatase-1 expression suppresses proinflammatory activation at sites that are resistant to atherosclerosis. *Circulation Research* **103,** 726–732 (2008).
50. Go, Y. M. *et al.* Phosphatidylinositol 3-kinase gamma mediates shear stress-dependent activation of JNK in endothelial cells. *Am. J. Physiol.* **275,** H1898–904 (1998).
51. Go, Y.-M. *et al.* Evidence for peroxynitrite as a signaling molecule in flow-dependent activation of c-Jun NH2-terminal kinase. *Am. J. Physiol. Heart Circ. Physiol.* **277,** H1647–H1653 (1999).
52. Go, Y. M. *et al.* Protein kinase B/Akt activates c-Jun NH(2)-terminal kinase by increasing NO production in response to shear stress. *J. Appl. Physiol.* **91,** 1574–1581 (2001).
53. Liu, P., Cheng, H., Roberts, T. M. & Zhao, J. J. Targeting the phosphoinositide 3-kinase pathway in cancer. *Nat Rev Drug Discov* **8,** 627–644 (2009).
54. Hers, I., Vincent, E. E. & Tavaré, J. M. Akt signalling in health and

disease. *Cell. Signal.* **23,** 1515–1527 (2011).
55. Dimmeler, S., Assmus, B., Hermann, C., Haendeler, J. & Zeiher, A. M. Fluid shear stress stimulates phosphorylation of Akt in human endothelial cells: involvement in suppression of apoptosis. *Circulation Research* **83,** 334–341 (1998).
56. Zachary, I. Focal adhesion kinase. *Int. J. Biochem. Cell Biol.* **29,** 929–934 (1997).
57. Mitra, S. K., Hanson, D. A. & Schlaepfer, D. D. Focal adhesion kinase: in command and control of cell motility. *Nat Rev Mol Cell Biol* **6,** 56–68 (2005).
58. Schlaepfer, D. D., Mitra, S. K. & Ilic, D. Control of motile and invasive cell phenotypes by focal adhesion kinase. *Biochim. Biophys. Acta* **1692,** 77–102 (2004).
59. Li, S. *et al.* The role of the dynamics of focal adhesion kinase in the mechanotaxis of endothelial cells. *Proc. Natl. Acad. Sci. U.S.A.* **99,** 3546–3551 (2002).
60. Cai, H., Liu, D. & Garcia, J. G. N. CaM Kinase II-dependent pathophysiological signalling in endothelial cells. *Cardiovascular Research* **77,** 30–34 (2008).
61. Balla, Z., Hoch, B., Karczewski, P. & Blasig, I. E. Calcium/calmodulin-dependent protein kinase IIdelta 2 and gamma isoforms regulate potassium currents of rat brain capillary endothelial cells under hypoxic conditions. *Journal of Biological Chemistry* **277,** 21306–21314 (2002).
62. Cai, H., Davis, M. E., Drummond, G. R. & Harrison, D. G. Induction of Endothelial NO Synthase by Hydrogen Peroxide via a Ca2+/Calmodulin-Dependent Protein Kinase II/Janus Kinase 2–Dependent Pathway. *Arterioscler Thromb Vasc Biol* **21,** 1571–1576 (2001).
63. Cai, H., McNally, J. S., Weber, M. & Harrison, D. G. Oscillatory shear stress upregulation of endothelial nitric oxide synthase requires intracellular hydrogen peroxide and CaMKII. *J. Mol. Cell. Cardiol.* **37,** 121–125 (2004).
64. Van Aelst, L. & D'Souza-Schorey, C. Rho GTPases and signaling networks. *Genes Dev.* **11,** 2295–2322 (1997).
65. Etienne-Manneville, S. & Hall, A. Rho GTPases in cell biology. *Nature* **420,** 629–635 (2002).
66. Lin, T. *et al.* Rho-ROCK-LIMK-cofilin pathway regulates shear stress activation of sterol regulatory element binding proteins. *Circulation Research* **92,** 1296–1304 (2003).

67. Tzima, E., del Pozo, M. A., Shattil, S. J., Chien, S. & Schwartz, M. A. Activation of integrins in endothelial cells by fluid shear stress mediates Rho-dependent cytoskeletal alignment. *EMBO J.* **20,** 4639–4647 (2001).
68. Li, S. *et al.* Distinct roles for the small GTPases Cdc42 and Rho in endothelial responses to shear stress. *J. Clin. Invest.* **103,** 1141–1150 (1999).
69. Wojciak-Stothard, B. & Ridley, A. J. Shear stress-induced endothelial cell polarization is mediated by Rho and Rac but not Cdc42 or PI 3-kinases. *J. Cell Biol.* **161,** 429–439 (2003).
70. Taylor, S. S. *et al.* PKA: a portrait of protein kinase dynamics. *Biochim. Biophys. Acta* **1697,** 259–269 (2004).
71. Boo, Y. C. *et al.* Shear stress stimulates phosphorylation of endothelial nitric-oxide synthase at Ser1179 by Akt-independent mechanisms: role of protein kinase A. *Journal of Biological Chemistry* **277,** 3388–3396 (2002).
72. Steinberg, S. F. Structural basis of protein kinase C isoform function. *Physiological Reviews* **88,** 1341–1378 (2008).
73. Newton, A. C. Protein kinase C: structure, function, and regulation. *Journal of Biological Chemistry* **270,** 28495–28498 (1995).
74. Hu, Y. L. & Chien, S. Effects of shear stress on protein kinase C distribution in endothelial cells. *J. Histochem. Cytochem.* **45,** 237–249 (1997).
75. Ni, C.-W. *et al.* Activation of PKC-epsilon and ERK1/2 participates in shear-induced endothelial MCP-1 expression that is repressed by nitric oxide. *J. Cell. Physiol.* **195,** 428–434 (2003).
76. Kuchan, M. J. & Frangos, J. A. Shear stress regulates endothelin-1 release via protein kinase C and cGMP in cultured endothelial cells. *Am. J. Physiol. Heart Circ. Physiol.* **264,** H150–H156 (1993).
77. Morita, T. *et al.* Role of Ca2+ and protein kinase C in shear stress-induced actin depolymerization and endothelin 1 gene expression. *Circulation Research* **75,** 630–636 (1994).
78. Ando, J., Nomura, H. & Kamiya, A. The effect of fluid shear stress on the migration and proliferation of cultured endothelial cells. *Microvascular Research* **33,** 62–70 (1987).
79. Levesque, M. J., Nerem, R. M. & Sprague, E. A. Vascular endothelial cell proliferation in culture and the influence of flow. *Biomaterials* **11,** 702–707 (1990).
80. Akimoto, S., Mitsumata, M., Sasaguri, T. & Yoshida, Y. Laminar shear stress inhibits vascular endothelial cell proliferation by

inducing cyclin-dependent kinase inhibitor p21(Sdi1/Cip1/Waf1). *Circulation Research* **86,** 185–190 (2000).
81. Lin, K. *et al.* Molecular mechanism of endothelial growth arrest by laminar shear stress. *Proc. Natl. Acad. Sci. U.S.A.* **97,** 9385–9389 (2000).
82. Chang, E. & Harley, C. B. Telomere length and replicative aging in human vascular tissues. *Proc. Natl. Acad. Sci. U.S.A.* **92,** 11190–11194 (1995).
83. Choy, J. C., Granville, D. J., Hunt, D. W. & McManus, B. M. Endothelial cell apoptosis: biochemical characteristics and potential implications for atherosclerosis. *J. Mol. Cell. Cardiol.* **33,** 1673–1690 (2001).
84. Ho, F. M. *et al.* Nitric oxide prevents apoptosis of human endothelial cells from high glucose exposure during early stage. *J. Cell. Biochem.* **75,** 258–263 (1999).
85. Dimmeler, S., Haendeler, J., Nehls, M. & Zeiher, A. M. Suppression of Apoptosis by Nitric Oxide via Inhibition of Interleukin-1β–converting Enzyme (ICE)-like and Cysteine Protease Protein (CPP)-32–like Proteases. *J. Exp. Med.* **185,** 601–608 (1997).
86. Heo, K.-S. *et al.* PKCζ mediates disturbed flow-induced endothelial apoptosis via p53 SUMOylation. *J. Cell Biol.* **193,** 867–884 (2011).
87. Jenkins, N. T. *et al.* Disturbed blood flow acutely induces activation and apoptosis of the human vascular endothelium. *Hypertension* **61,** 615–621 (2013).
88. Michaelis, U. R. Mechanisms of endothelial cell migration. *Cell. Mol. Life Sci.* **71,** 4131–4148 (2014).
89. Lamalice, L., Le Boeuf, F. & Huot, J. Endothelial cell migration during angiogenesis. *Circulation Research* (2007). doi:10.1161/01.RES.0000259593.07661.1e
90. Albuquerque, M. L., Waters, C. M., Savla, U., Schnaper, H. W. & Flozak, A. S. Shear stress enhances human endothelial cell wound closure in vitro. *Am. J. Physiol. Heart Circ. Physiol.* **279,** H293–302 (2000).
91. Hu, Y. L., Li, S., Miao, H., Tsou, T. C. & del Pozo, M. A. Roles of microtubule dynamics and small GTPase Rac in endothelial cell migration and lamellipodium formation under flow. *Journal of vascular …* (2002). doi:10.1159/000067202
92. Tzima, E. Role of small GTPases in endothelial cytoskeletal dynamics and the shear stress response. *Circulation Research* **98,** 176–185 (2006).

93. Romer, L. H., McLean, N. & Turner, C. E. Tyrosine kinase activity, cytoskeletal organization, and motility in human vascular endothelial cells. *Molecular Biology of the …* (1994).
94. Gilmore, A. P. & Romer, L. H. Inhibition of focal adhesion kinase (FAK) signaling in focal adhesions decreases cell motility and proliferation. *Mol. Biol. Cell* **7,** 1209–1224 (1996).
95. Urbich, C. *et al.* Shear stress-induced endothelial cell migration involves integrin signaling via the fibronectin receptor subunits alpha(5) and beta(1). *Arterioscler Thromb Vasc Biol* **22,** 69–75 (2002).
96. Galis, Z., Ghitescu, L. & Simionescu, M. Fatty acids binding to albumin increases its uptake and transcytosis by the lung capillary endothelium. *Eur J Cell Biol* **47,** 358–365 (1988).
97. Mehta, D. & Malik, A. B. Signaling mechanisms regulating endothelial permeability. *Physiological Reviews* **86,** 279–367 (2006).
98. Nielsen, L. B., Nordestgaard, B. G., Stender, S. & Kjeldsen, K. Aortic permeability to LDL as a predictor of aortic cholesterol accumulation in cholesterol-fed rabbits. *Arterioscler. Thromb.* **12,** 1402–1409 (1992).
99. Herrmann, R. A., Malinauskas, R. A. & Truskey, G. A. Characterization of sites with elevated LDL permeability at intercostal, celiac, and iliac branches of the normal rabbit aorta. *Arterioscler. Thromb.* **14,** 313–323 (1994).
100. Bell, F. P., Adamson, I. L. & Schwartz, C. J. Aortic endothelial permeability to albumin: focal and regional patterns of uptake and transmural distribution of 131I-albumin in the young pig. *Experimental and molecular pathology* **20,** 57–68 (1974).
101. Himburg, H. A. *et al.* Spatial comparison between wall shear stress measures and porcine arterial endothelial permeability. *Am. J. Physiol. Heart Circ. Physiol.* **286,** H1916–22 (2004).
102. Baldwin, A. L., Thurston, G. & Naemi, al, H. Inhibition of nitric oxide synthesis increases venular permeability and alters endothelial actin cytoskeleton. *Am. J. Physiol.* **274,** H1776–84 (1998).
103. Draijer, R., Atsma, D. E., van der Laarse, A. & van Hinsbergh, V. W. cGMP and nitric oxide modulate thrombin-induced endothelial permeability. Regulation via different pathways in human aortic and umbilical vein endothelial cells. *Circulation Research* **76,** 199–208 (1995).
104. Tarbell, J. M., Demaio, L. & Zaw, M. M. Effect of pressure on hydraulic conductivity of endothelial monolayers: role of endothelial

cleft shear stress. *J. Appl. Physiol.* **87,** 261–268 (1999).
105. Davies, P. F., Robotewskyj, A. & Griem, M. L. Quantitative studies of endothelial cell adhesion. Directional remodeling of focal adhesion sites in response to flow forces. *J. Clin. Invest.* **93,** 2031–2038 (1994).
106. Dewey, C. F., Bussolari, S. R., Gimbrone, M. A. & Davies, P. F. The dynamic response of vascular endothelial cells to fluid shear stress. *J Biomech Eng* **103,** 177–185 (1981).
107. Malek, A. M. & Izumo, S. Mechanism of endothelial cell shape change and cytoskeletal remodeling in response to fluid shear stress. *J. Cell. Sci.* **109 (Pt 4),** 713–726 (1996).
108. Nerem, R. M., Levesque, M. J. & Cornhill, J. F. Vascular endothelial morphology as an indicator of the pattern of blood flow. *J Biomech Eng* **103,** 172–176 (1981).
109. Remuzzi, A., Dewey, C. F., Davies, P. F. & Gimbrone, M. A. Orientation of endothelial cells in shear fields in vitro. *Biorheology* **21,** 617–630 (1984).
110. Wechezak, A. R., Viggers, R. F. & Sauvage, L. R. Fibronectin and F-actin redistribution in cultured endothelial cells exposed to shear stress. *Lab. Invest.* **53,** 639–647 (1985).
111. Galbraith, C. G., Skalak, R. & Chien, S. Shear stress induces spatial reorganization of the endothelial cell cytoskeleton. *Cell Motility and the Cytoskeleton* **40,** 317–330 (1998).
112. Shen, J., Luscinskas, F. W., Connolly, A., Dewey, C. F. & Gimbrone, M. A. Fluid shear stress modulates cytosolic free calcium in vascular endothelial cells. *Am. J. Physiol.* **262,** C384–90 (1992).
113. Geiger, R. V., Berk, B. C., Alexander, R. W. & Nerem, R. M. Flow-induced calcium transients in single endothelial cells: spatial and temporal analysis. *Am. J. Physiol.* **262,** C1411–7 (1992).
114. Prasad, A. R., Logan, S. A., Nerem, R. M., Schwartz, C. J. & Sprague, E. A. Flow-related responses of intracellular inositol phosphate levels in cultured aortic endothelial cells. *Circulation Research* **72,** 827–836 (1993).
115. Lu, D. & Kassab, G. S. Role of shear stress and stretch in vascular mechanobiology. *Journal of The Royal Society Interface* **8,** 1379–1385 (2011).
116. Ignarro, L. J., Buga, G. M., Wood, K. S., Byrns, R. E. & Chaudhuri, G. Endothelium-derived relaxing factor produced and released from artery and vein is nitric oxide. *Proc. Natl. Acad. Sci. U.S.A.* **84,** 9265–9269 (1987).

117. Böhm, F. & Pernow, J. The importance of endothelin-1 for vascular dysfunction in cardiovascular disease. *Cardiovascular Research* **76,** 8–18 (2007).
118. Dinh-Xuan, A. T. Endothelial modulation of pulmonary vascular tone. *Eur. Respir. J.* **5,** 757–762 (1992).
119. Murad, F. Cyclic guanosine monophosphate as a mediator of vasodilation. *J. Clin. Invest.* **78,** 1–5 (1986).
120. Yanagisawa, M., Kurihara, H., Kimura, S. & Tomobe, Y. A novel potent vasoconstrictor peptide produced by vascular endothelial cells. *Nature* (1988).
121. Van Renterghem, C., Vigne, P. & Barhanin, J. Molecular mechanism of action of the vasoconstrictor peptide endothelin. *Biochemical and …* **157,** 977–985 (1988).
122. Frangos, J. A., Eskin, S. G., McIntire, L. V. & Ives, C. L. Flow effects on prostacyclin production by cultured human endothelial cells. *Science* **227,** 1477–1479 (1985).
123. Pearce, M. J., McIntyre, T. M. & Prescott, S. M. Shear stress activates cytosolic phospholipase A 2 (cPLA 2) and MAP kinase in human endothelial cells. *Biochemical and …* **218,** 500–504 (1996).
124. Okahara, K., Sun, B. & Kambayashi, J. Upregulation of prostacyclin synthesis-related gene expression by shear stress in vascular endothelial cells. *Arterioscler Thromb Vasc Biol* **18,** 1922–1926 (1998).
125. Humphrey, J. D., Schwartz, M. A., Tellides, G. & Milewicz, D. M. Role of mechanotransduction in vascular biology: focus on thoracic aortic aneurysms and dissections. *Circulation Research* **116,** 1448–1461 (2015).
126. Brown, A. J. *et al.* Role of biomechanical forces in the natural history of coronary atherosclerosis. *Nat Rev Cardiol* **13,** 210–220 (2016).
127. Shao, J.-S., Cai, J. & Towler, D. A. Molecular mechanisms of vascular calcification: lessons learned from the aorta. *Arterioscler Thromb Vasc Biol* **26,** 1423–1430 (2006).
128. Glass, C. K. & Witztum, J. L. Atherosclerosis: the road ahead. *Cell* **104,** 503–516 (2001).
129. Asakura, T. & Karino, T. Flow patterns and spatial distribution of atherosclerotic lesions in human coronary arteries. *Circulation Research* **66,** 1045–1066 (1990).
130. Malek, A. M., Alper, S. L. & Izumo, S. Hemodynamic shear stress and its role in atherosclerosis. *JAMA* **282,** 2035–2042 (1999).
131. Fry, D. L. Certain histological and chemical responses of the

vascular interface to acutely induced mechanical stress in the aorta of the dog. *Circulation Research* **24,** 93–108 (1969).
132. Caro, C. G., Fitz-Gerald, J. M. & Schroter, R. C. Atheroma and arterial wall shear. Observation, correlation and proposal of a shear dependent mass transfer mechanism for atherogenesis. *Proc. R. Soc. Lond., B, Biol. Sci.* **177,** 109–159 (1971).
133. Zarins, C. K. *et al.* Carotid bifurcation atherosclerosis. Quantitative correlation of plaque localization with flow velocity profiles and wall shear stress. *Circulation Research* **53,** 502–514 (1983).
134. Sawchuk, A. P., Unthank, J. L., Davis, T. E. & Dalsing, M. C. A prospective, in vivo study of the relationship between blood flow hemodynamics and atherosclerosis in a hyperlipidemic swine model. *J. Vasc. Surg.* **19,** 58–63– discussion 63–4 (1994).
135. Gnasso, A. *et al.* In vivo association between low wall shear stress and plaque in subjects with asymmetrical carotid atherosclerosis. *Stroke* **28,** 993–998 (1997).
136. Cheng, C. *et al.* Atherosclerotic lesion size and vulnerability are determined by patterns of fluid shear stress. *Circulation* **113,** 2744–2753 (2006).
137. Cheng, C. *et al.* Shear stress affects the intracellular distribution of eNOS: direct demonstration by a novel in vivo technique. *Blood* **106,** 3691–3698 (2005).
138. Harrison, D. G. *et al.* Endothelial mechanotransduction, nitric oxide and vascular inflammation. *J. Intern. Med.* **259,** 351–363 (2006).
139. DePaola, N. *et al.* Spatial and temporal regulation of gap junction connexin43 in vascular endothelial cells exposed to controlled disturbed flows in vitro. *Proc. Natl. Acad. Sci. U.S.A.* **96,** 3154–3159 (1999).
140. Miao, H. *et al.* Effects of flow patterns on the localization and expression of VE-cadherin at vascular endothelial cell junctions: in vivo and in vitro investigations. *J. Vasc. Res.* **42,** 77–89 (2005).
141. Ley, K., Laudanna, C., Cybulsky, M. I. & Nourshargh, S. Getting to the site of inflammation: the leukocyte adhesion cascade updated. *Nat Rev Immunol* **7,** 678–689 (2007).
142. S Björkerud, B. B. Apoptosis is abundant in human atherosclerotic lesions, especially in inflammatory cells (macrophages and T cells), and may contribute to the accumulation of gruel and plaque instability. *The American Journal of Pathology* **149,** 367–380 (1996).
143. Chiu, J.-J. *et al.* Shear stress increases ICAM-1 and decreases VCAM-1 and E-selectin expressions induced by tumor necrosis

factor-[alpha] in endothelial cells. *Arterioscler Thromb Vasc Biol* **24,** 73–79 (2004).
144. Chappell, D. C., Varner, S. E., Nerem, R. M., Medford, R. M. & Alexander, R. W. Oscillatory shear stress stimulates adhesion molecule expression in cultured human endothelium. *Circulation Research* **82,** 532–539 (1998).
145. Nagel, T., Resnick, N. & Dewey, C. F. Vascular endothelial cells respond to spatial gradients in fluid shear stress by enhanced activation of transcription factors. *…* (1999).
146. Hahn, C., Orr, A. W., Sanders, J. M., Jhaveri, K. A. & Schwartz, M. A. The subendothelial extracellular matrix modulates JNK activation by flow. *Circulation Research* **104,** 995–1003 (2009).
147. Schwenke, D. C. & Carew, T. E. Initiation of atherosclerotic lesions in cholesterol-fed rabbits. I. Focal increases in arterial LDL concentration precede development of fatty streak lesions. *Arteriosclerosis* **9,** 895–907 (1989).
148. Suo, J., Oshinski, J. N. & Giddens, D. P. Blood flow patterns in the proximal human coronary arteries: relationship to atherosclerotic plaque occurrence. *Mol Cell Biomech* **5,** 9–18 (2008).
149. Schwenke, D. C. & Carew, T. E. Initiation of atherosclerotic lesions in cholesterol-fed rabbits. II. Selective retention of LDL vs. selective increases in LDL permeability in susceptible sites of arteries. *Arteriosclerosis* **9,** 908–918 (1989).
150. Murase, T. *et al.* Fluid shear stress transcriptionally induces lectin-like oxidized LDL receptor-1 in vascular endothelial cells. *Circulation Research* **83,** 328–333 (1998).
151. Weber, C. & Noels, H. Atherosclerosis: current pathogenesis and therapeutic options. *Nature Medicine* **17,** 1410–1422 (2011).
152. Tinken, T. M. *et al.* Shear stress mediates endothelial adaptations to exercise training in humans. *Hypertension* **55,** 312–318 (2010).
153. Schuler, G., Adams, V. & Goto, Y. Role of exercise in the prevention of cardiovascular disease: results, mechanisms, and new perspectives. *European Heart Journal* **34,** 1790–1799 (2013).
154. Topper, J. N. & Gimbrone, M. A. Blood flow and vascular gene expression: fluid shear stress as a modulator of endothelial phenotype. *Mol Med Today* **5,** 40–46 (1999).
155. Chien, S. Mechanotransduction and endothelial cell homeostasis: the wisdom of the cell. *Am. J. Physiol. Heart Circ. Physiol.* **292,** H1209–H1224 (2006).
156. Ando, J. *et al.* Shear stress inhibits adhesion of cultured mouse

endothelial cells to lymphocytes by downregulating VCAM-1 expression. *Am. J. Physiol.* **267,** C679–87 (1994).
157. Malek, A. M., Greene, A. L. & Izumo, S. Regulation of endothelin 1 gene by fluid shear stress is transcriptionally mediated and independent of protein kinase C and cAMP. *Proc. Natl. Acad. Sci. U.S.A.* **90,** 5999–6003 (1993).
158. Dimmeler, S., Haendeler, J., Rippmann, V., Nehls, M. & Zeiher, A. M. Shear stress inhibits apoptosis of human endothelial cells. *FEBS Lett.* **399,** 71–74 (1996).
159. Topper, J. N., Cai, J., Falb, D. & Gimbrone, M. A. Identification of vascular endothelial genes differentially responsive to fluid mechanical stimuli: cyclooxygenase-2, manganese superoxide dismutase, and endothelial cell nitric oxide synthase are selectively up-regulated by steady laminar shear stress. *Proc. Natl. Acad. Sci. U.S.A.* **93,** 10417–10422 (1996).
160. Lin, Z. *et al.* Kruppel-like factor 2 (KLF2) regulates endothelial thrombotic function. *Circulation Research* **96,** e48–57 (2005).
161. Dekker, R. J. *et al.* Prolonged fluid shear stress induces a distinct set of endothelial cell genes, most specifically lung Krüppel-like factor (KLF2). *Blood* **100,** 1689–1698 (2002).
162. Dekker, R. J. *et al.* Endothelial KLF2 links local arterial shear stress levels to the expression of vascular tone-regulating genes. *The American Journal of Pathology* **167,** 609–618 (2005).
163. Chien, S. Effects of Disturbed Flow on Endothelial Cells. *Ann Biomed Eng* **36,** 554–562 (2008).
164. Fukushima, T., Karino, T. & Goldsmith, H. L. Disturbances of flow through transparent dog aortic arch. *Heart Vessels* **1,** 24–28 (1985).
165. Beere, P. A., Glagov, S. & Zarins, C. K. Experimental atherosclerosis at the carotid bifurcation of the cynomolgus monkey. Localization, compensatory enlargement, and the sparing effect of lowered heart rate. *Arterioscler. Thromb.* **12,** 1245–1253 (1992).
166. Gnasso, A. *et al.* Association between intima-media thickness and wall shear stress in common carotid arteries in healthy male subjects. *Circulation* **94,** 3257–3262 (1996).
167. Brooks, A. R., Lelkes, P. I. & Rubanyi, G. M. Gene expression profiling of human aortic endothelial cells exposed to disturbed flow and steady laminar flow. *Physiol Genomics* **9,** 27–41 (2002).
168. Ni, C. W. *et al.* Discovery of novel mechanosensitive genes in vivo using mouse carotid artery endothelium exposed to disturbed flow. *Blood* **116,** e66–e73 (2010).

169. Chen, B. P. *et al.* DNA microarray analysis of gene expression in endothelial cells in response to 24-h shear stress. *Physiol Genomics* **7,** 55–63 (2001).
170. García-Cardeña, G., Comander, J., Anderson, K. R., Blackman, B. R. & Gimbrone, M. A. Biomechanical activation of vascular endothelium as a determinant of its functional phenotype. *Proc. Natl. Acad. Sci. U.S.A.* **98,** 4478–4485 (2001).
171. Mortazavi, A., Williams, B. A., McCue, K., Schaeffer, L. & Wold, B. Mapping and quantifying mammalian transcriptomes by RNA-Seq. *Nat Meth* **5,** 621–628 (2008).
172. Mercer, T. R., Dinger, M. E. & Mattick, J. S. Long non-coding RNAs: insights into functions. *Nat Rev Genet* **10,** 155–159 (2009).
173. Lander, E. S. *et al.* Initial sequencing and analysis of the human genome. *Nature* **409,** 860–921 (2001).
174. Ohno, S. So much 'junk' DNA in our genome. *Brookhaven Symp. Biol.* **23,** 366–370 (1972).
175. Filipowicz, W., Bhattacharyya, S. N. & Sonenberg, N. Mechanisms of post-transcriptional regulation by microRNAs: are the answers in sight? *Nat Rev Genet* **9,** 102–114 (2008).
176. Whitehead, J., Pandey, G. K. & Kanduri, C. Regulation of the mammalian epigenome by long noncoding RNAs. *Biochim. Biophys. Acta* **1790,** 936–947 (2009).
177. Cech, T. R. & Steitz, J. A. The Noncoding RNA Revolution—Trashing Old Rules to Forge New Ones. **157,** 77–94 (2014).
178. Baker, M. Long noncoding RNAs: the search for function. *Nat Meth* (2011). doi:10.1038/nmeth0511-379
179. Puthanveetil, P., Chen, S., Feng, B., Gautam, A. & Chakrabarti, S. Long non-coding RNA MALAT1 regulates hyperglycaemia induced inflammatory process in the endothelial cells. *J. Cell. Mol. Med.* (2015). doi:10.1111/jcmm.12576
180. Hove, J. R. *et al.* Intracardiac fluid forces are an essential epigenetic factor for embryonic cardiogenesis. *Nature* **421,** 172–177 (2003).
181. Freedman, L. P., Cockburn, I. M. & Simcoe, T. S. The Economics of Reproducibility in Preclinical Research. *PLoS Biol.* **13,** e1002165 (2015).
182. Wang, Z., Gerstein, M. & Snyder, M. RNA-Seq: a revolutionary tool for transcriptomics. *Nat Rev Genet* **10,** 57–63 (2009).
183. Takai, J. *et al.* Laminar shear stress upregulates endothelial Ca^{2+}-activated K^+ channels KCa2.3 and KCa3.1 via a Ca^{2+}/calmodulin-dependent protein kinase kinase/Akt/p300 cascade. *Am. J. Physiol.*

Heart Circ. Physiol. **305,** H484–H493 (2013).
184. Liao, Y., Smyth, G. K. & Shi, W. The Subread aligner: fast, accurate and scalable read mapping by seed-and-vote. *Nucleic Acids Research* **41,** e108 (2013).
185. Ritchie, M. E. *et al.* limma powers differential expression analyses for RNA-sequencing and microarray studies. *Nucleic Acids Research* **43,** e47 (2015).
186. Honda, H. M. *et al.* A complex flow pattern of low shear stress and flow reversal promotes monocyte binding to endothelial cells. *Atherosclerosis* **158,** 385–390 (2001).
187. Cines, D. B. *et al.* Endothelial cells in physiology and in the pathophysiology of vascular disorders. *Blood* **91,** 3527–3561 (1998).
188. Go, Y. M., Boo, Y. C., Park, H. & Maland, M. C. Protein kinase B/Akt activates c-Jun NH2-terminal kinase by increasing NO production in response to shear stress. *Journal of Applied …* (2001).
189. Michalik, K. M. *et al.* Long Noncoding RNA MALAT1 Regulates Endothelial Cell Function and Vessel Growth. *Circulation Research* **114,** 1389–1397 (2014).
190. Tripathi, V. *et al.* Long Noncoding RNA MALAT1 Controls Cell Cycle Progression by Regulating the Expression of Oncogenic Transcription Factor B-MYB. *PLoS Genet* **9,** e1003368 (2013).
191. Mozaffarian, D. *et al.* Heart disease and stroke statistics--2015 update: a report from the American Heart Association. *Circulation* **131,** e29–322 (2015).
192. Gimbrone, M. A. & García-Cardeña, G. Endothelial Cell Dysfunction and the Pathobiology of Atherosclerosis. *Circulation Research* **118,** 620–636 (2016).
193. Pasceri, V., Willerson, J. T. & Yeh, E. Direct proinflammatory effect of C-reactive protein on human endothelial cells. *Circulation* (2000).
194. Carlos, T. M. & Harlan, J. M. Leukocyte-endothelial adhesion molecules. *Blood* **84,** 2068–2101 (1994).
195. Simionescu, N., Vasile, E., Lupu, F. & Popescu, G. *Accumulation of extracellular cholesterol-rich liposomes in the arterial intima and cardiac valves of the hyperlipidemic rabbit*. (Am J Pathol, 1986).
196. Ross, R. & Glomset, J. A. Atherosclerosis and the arterial smooth muscle cell: Proliferation of smooth muscle is a key event in the genesis of the lesions of atherosclerosis. *Science* **180,** 1332–1339 (1973).
197. Cybulsky, M. I. & Gimbrone, M. A. Endothelial expression of a mononuclear leukocyte adhesion molecule during atherogenesis.

Science **251,** 788–791 (1991).
198. Thüsen, von der, J. H., van Berkel, T. J. & Biessen, E. A. Induction of rapid atherogenesis by perivascular carotid collar placement in apolipoprotein E-deficient and low-density lipoprotein receptor-deficient mice. *Circulation* **103,** 1164–1170 (2001).
199. Calandra, T. & Roger, T. Macrophage migration inhibitory factor: a regulator of innate immunity. *Nat Rev Immunol* **3,** 791–800 (2003).
200. Lin, S. G. *et al.* De novo expression of macrophage migration inhibitory factor in atherogenesis in rabbits. *Circulation Research* **87,** 1202–1208 (2000).
201. Burger-Kentischer, A., Goebel, H., Seiler, R. & Fraedrich, G. Expression of macrophage migration inhibitory factor in different stages of human atherosclerosis. *Circulation* (2002). doi:10.1161/01.CIR.0000012942.49244.82
202. Pan, J.-H. *et al.* Macrophage migration inhibitory factor deficiency impairs atherosclerosis in low-density lipoprotein receptor-deficient mice. *Circulation* **109,** 3149–3153 (2004).
203. Burger-Kentischer, A. *et al.* Reduction of the aortic inflammatory response in spontaneous atherosclerosis by blockade of macrophage migration inhibitory factor (MIF). *Atherosclerosis* **184,** 28–38 (2006).
204. Bernhagen, J. *et al.* MIF is a noncognate ligand of CXC chemokine receptors in inflammatory and atherogenic cell recruitment. *Nature Medicine* **13,** 587–596 (2007).
205. Nishihira, J., Koyama, Y. & Mizue, Y. Identification of macrophage migration inhibitory factor (MIF) in human vascular endothelial cells and its induction by lipopolysaccharide. *Cytokine* **10,** 199–205 (1998).
206. Cheng, Q. *et al.* Macrophage migration inhibitory factor increases leukocyte-endothelial interactions in human endothelial cells via promotion of expression of adhesion molecules. *J. Immunol.* **185,** 1238–1247 (2010).
207. Iyer, M. K. *et al.* The landscape of long noncoding RNAs in the human transcriptome. 1–13 (2015). doi:10.1038/ng.3192
208. Caro, C. G., Fitz-Gerald, J. M. & Schroter, R. C. Arterial wall shear and distribution of early atheroma in man. *Nature* **223,** 1159–1160 (1969).
209. Atkins, G. B. & Jain, M. K. Role of Krüppel-like transcription factors in endothelial biology. *Circulation Research* **100,** 1686–1695 (2007).
210. Fan, Y. *et al.* Kruppel-Like Factor-11, a Transcription Factor Involved

in Diabetes Mellitus, Suppresses Endothelial Cell Activation via the Nuclear Factor-κB Signaling Pathway. *Arterioscler Thromb Vasc Biol* **32,** 2981–2988 (2012).
211. Hamik, A. *et al.* Kruppel-like factor 4 regulates endothelial inflammation. *Journal of Biological Chemistry* **282,** 13769–13779 (2007).
212. Association, A. H. *Heart disease and stroke statistics—at a glance*. (2015).
213. Schmeisser, A. *et al.* The expression of macrophage migration inhibitory factor 1alpha (MIF 1alpha) in human atherosclerotic plaques is induced by different proatherogenic stimuli and associated with plaque instability. *Atherosclerosis* **178,** 83–94 (2005).
214. Schober, A. *et al.* Stabilization of atherosclerotic plaques by blockade of macrophage migration inhibitory factor after vascular injury in apolipoprotein E-deficient mice. *Circulation* **109,** 380–385 (2004).
215. Lee, J. S. *et al.* Klf2 is an essential regulator of vascular hemodynamic forces in vivo. *Dev. Cell* **11,** 845–857 (2006).
216. Zhang, J. & Friedman, M. H. Adaptive response of vascular endothelial cells to an acute increase in shear stress magnitude. *AJP: Heart and Circulatory Physiology* **302,** H983–91 (2012).
217. Bartel, D. P. MicroRNAs: target recognition and regulatory functions. *Cell* **136,** 215–233 (2009).
218. Marin, T. *et al.* Mechanosensitive microRNAs-role in endothelial responses to shear stress and redox state. *Free Radical Biology and Medicine* **64,** 61–68 (2013).
219. Kumar, S., Kim, C. W., Simmons, R. D. & Jo, H. Role of flow-sensitive microRNAs in endothelial dysfunction and atherosclerosis: mechanosensitive athero-miRs. *Arterioscler Thromb Vasc Biol* **34,** 2206–2216 (2014).
220. Davis, M. E., Cai, H. & Drummond, G. R. Shear stress regulates endothelial nitric oxide synthase expression through c-Src by divergent signaling pathways. *Circulation Research* (2001). doi:10.1161/hh2301.100806
221. Felcht, M. *et al.* Angiopoietin-2 differentially regulates angiogenesis through TIE2 and integrin signaling. *J. Clin. Invest.* **122,** 1991–2005 (2012).
222. Endo, A. A historical perspective on the discovery of statins. in (2010). doi:10.2183/pjab.86.484

223. Blackman, B. R. A new in vitro model to evaluate differential responses of endothelial cells to simulated arterial shear stress waveforms. *Journal of …* (2002). doi:10.1115/1.1486468
224. Adamo, L. *et al.* Biomechanical forces promote embryonic haematopoiesis. *Nature* **459,** 1131–1135 (2009).
225. Paz, dela, N. G., Walshe, T. E., Leach, L. L., Saint-Geniez, M. & D'Amore, P. A. Role of shear-stress-induced VEGF expression in endothelial cell survival. *J. Cell. Sci.* **125,** 831–843 (2012).
226. Settembre, C. *et al.* TFEB links autophagy to lysosomal biogenesis. *Science* **332,** 1429–1433 (2011).
227. Kumarswamy, R. *et al.* Circulating Long Noncoding RNA, LIPCAR, Predicts Survival in Patients With Heart Failure. *Circulation Research* **114,** 1569–1575 (2014).
228. Han, P. *et al.* A long noncoding RNA protects the heart from pathological hypertrophy. *Nature* **514,** 102–106 (2014).